OPEN GEOMECHANICS

Introductory consideration supporting the idea of the release of elastic waves in hysteretic soil

Piotr Kowalczyk [a] *& Alessandro Gajo* [b]

[a] *University of Southampton, Faculty of Engineering and Physical Sciences, Southampton, United Kingdom*

[b] *University of Trento, Department of Civil, Environmental and Mechanical Engineering, Trento, Italy.*

Published
22nd January 2024
https://doi.org/10.5802/ogeo.16

Edited by
Benjy Marks
School of Civil Engineering
The University of Sydney
Australia

Reviewed by
Max Wiebicke
School of Civil Engineering
The University of Sydney
Australia

Saif Alzabeebee
Department of Roads and Transport Engineering
College of Engineering
University of Al-Qadisiyah
Iraq

One anonymous reviewer

Correspondence
Piotr Kowalczyk
University of Southampton, Faculty of Engineering and Physical Sciences, Boldrewood Campus Southampton, United Kingdom
p.kowalczyk@soton.ac.uk

Open Geomechanics is member of the Centre Mersenne for Open Scientific Publishing

Abstract. Unintended and unwanted high frequency motion is sometimes observed in small-scale experimental works and in numerical simulations when soil is subjected to simple harmonic input motions. This high frequency motion has been often attributed to the drawbacks of actuating systems in experimental setups and to numerical noise in computational analyses. This work presents introductory consideration supporting the hypothetical idea that the recorded and the computed high frequency motion can possibly be the consequence of an unrecognized before physical phenomenon of soil elastic waves released in nonlinear hysteretic soil and affecting the dynamic response of soil to harmonic excitation. To this aim, simplified numerical studies representative of the most basic soil mechanical properties are carried out. The results reveal potential importance of soil-released elastic waves and their reflections inside a soil column when understanding the free field response in the numerical simulations representative of small-scale experimental setups. Chosen numerical cases are compared with available examples of experimental works from the literature. In addition, two further cases are analyzed, including a case showing the potential importance of soil-released elastic waves in the response of soil to real earthquakes, and a case showing the response of structural elements.

Keywords. Soil dynamics, elastic waves, wave propagation, soil nonlinearity, finite element modelling, soil constitutive modelling

1. Introduction

The recent advances in seismic geotechnical engineering are achieved by high quality small-scale experimental works and advanced numerical studies. The most important aims of the physical modelling are twofold: improved understanding of soil-structure interaction during seismic events and creating reference baseline for validation of numerical modelling studies, thus, allowing their use in subsequent predictive studies of full-scale problems. Although advanced physical and numerical modelling are considered as reliable ways of investigating seismic behaviour of soil, both these methodologies are often affected by the presence of unexpected high frequency oscillations in recorded or computed motions.

Physical modelling of soil seismic behaviour is typically achieved in flexible soil containers placed on shaking tables in 1g (e.g. [Durante et al., 2016]) or centrifuge (multiple g) experimental setups (e.g. [Lanzano et al., 2012]). Such experimental studies often record unexpected and undesired high frequency content even though they use simplified sinusoidal input motions of a single frequency applied at base. For example, high frequency content in a form of a regular pattern of higher harmonics, i.e. 3ω, 5ω, 7ω etc. (where ω is the driving frequency), was observed by many research centres participating in the LEAP-GWU-2015 [Kutter et al., 2018] and LEAP-UCD-2017 [Kutter et al., 2019] projects on saturated soil slopes. Experimental work on dry soil also revealed the presence of undesired high harmonics for intended perfect sinusoidal input motions (e.g. [Lanzano et al., 2012, Conti and Viggiani, 2012], [Conti et al., 2012], [Abate and Massimino, 2016]). Sometimes the high harmonics of a regular pattern 3ω, 5ω, 7ω etc. were also recorded at base level. For example, Madabhushi [2014] showed example input motion recorded at base in a centrifuge test to comprise harmonics in the regular form of ω, 3ω, 5ω, 7ω etc. As a result of this observation, the presence of high harmonics is often attributed to the actuating systems (e.g. [Brennan et al., 2005]). In more detail, Kutter et al. [2018] and Manandhar et al. [2021] indicated difficulties in controlling high frequency content in actuators, Lanzano et al. [2012] pointed out at potential resonance with higher vibration modes of the shakers, whereas Yao et al. [2017] showed that high harmonics are recorded on an empty shaking table for very high amplitude input motions and they attributed these high harmonics to non-linearities in the actuating system.

The presence of high frequency content recorded in experimental works has also been explained as a result of physical phenomena. In studies regarding saturated soil, high frequency content could be associated with "deliquefaction shock waves" [Kutter and Wilson, 1999] or in other words with dilation, sudden reduction in excess pore pressure and consequent sudden increase in soil stiffness (e.g. [Bonilla et al., 2005], [Roten et al., 2013], [McAllister et al., 2015], [Wang et al., 2018]). On the other hand, high frequencies occurring in experimental setups containing dry soil were attempted to be explained by "soil fluidisation" [Dar, 1993], shear band development at shallow soil depths [Gajo and Muir Wood, 1997] or attributed to be a proof of pounding between soil and piles [Chau et al., 2009]. In general, one is reminded that any nonlinearity in a physical system is expected to generate high harmonics for a single driving frequency of ω (e.g. [Nekorkin, 2015]). For instance, high harmonics for perfect sine input motion were observed in frictional base isolation systems (e.g. [Kelly, 1982], [Fan et al., 1988], [Wiebe and Christopoulos, 2010]) or in a harmonic oscillator with sliding friction [Vitorino et al., 2017]. In the latter work abrupt changes in stiffness and changes in the direction of the friction force induced nonlinearity and led to the generation of high frequency motion of the oscillator. Some numerical studies in the past showed that soil inherent nonlinearity can also generate high harmonics for single sine input motions [Pavlenko, 2001], [Pavlenko and Irikura, 2005], [Mercado et al., 2018], [Veeraraghavan et al., 2019]. In more detail, Pavlenko [2001] and Pavlenko and Irikura [2005] used a simple hysteretic soil model and monochromatic seismic input motions to show regular high frequency patterns for an example soil profile and for the 1995 Kobe earthquake site, respectively. A recent study by Mercado et al. [2018] showed similar conclusions with the amount of harmonics being dependent on the level of nonlinearity based on comparisons of experimental data from centrifuge on saturated soil with single-phase numerical simulations obtained with a simplified hyperbolic, backbone soil model. The presence of high harmonics was shown to follow the pattern of exponential decay in the amount of the consecutive harmonics as a result of the distortion of a sinusoidal wave towards a square wave. Finally, Veeraraghavan et al. [2019] approximated a soil column as a single nonlinear element without considering wave propagation and showed that the shape of the stress-strain hysteresis determines the presence of high frequency components. To sum up, some physical explanations to the observed high harmonics have been shown by the previous studies, however the theoretical analyses proposed so far are not fully consistent with each other and do not include suitable comparisons with experimental evidence. Moreover, these studies explain only the presence of high frequency components occurring in the evaluated spectral responses; however, they do not explain the origin of the potential presence of additional waves generated in soil.

The occurrence of high frequency content appears also in numerical studies. For instance, the performance of the numerical models in the LEAP-UCD-2017 project was presented by Manzari et al. [2019]. This study highlighted the fact that some constitutive models were able to represent the high frequency content in a similar way as obtained in the centrifuge tests, whereas some other constitutive models were able to damp out high frequencies. The presence or absence of high harmonics was attributed more to the implemented numerical or viscous damping and less to the constitutive models themselves. To the best of the Authors' knowledge, majority of the predicting teams used the signal recorded in the centrifuge tests at the base of the soil container as input motion in the computations, thus, including high harmonics. Similarly, Bilotta et al.

[2014] showed that different predicting teams chose different methods to remove, considered as spurious, high frequencies e.g. by means of result filtering or application of viscous damping, and were able to obtain comparable response spectra at soil surface with experimental data. A more specific study, dealing strictly with the occurrence of high frequency content in numerical studies, was presented by Tsiapas and Bouckovalas [2018]. They observed that the source of the high frequency spikes can be attributed to "abrupt stiffness changes due to dilation and/or unloading-reloading", attributed such frequencies to numerical noise and proposed a filtering method to remove such noise from the computations of dry and saturated soil.

The problem of high frequency content appears in both, physical and numerical modelling studies. This paper shows a potential new explanation to the source of such high frequencies based on the hypothetical idea of the release of soil elastic waves in nonlinear hysteretic soil where unloading waves propagate. In general, the importance of unloading waves is well recognized in solid mechanics (e.g. [Nowacki, 1978], [Wang, 2007]). On the other hand, the importance of unloading waves in wave propagation in soil has not been studied explicitly. Some very initial numerical studies on the effects of unloading waves were limited only to a soil column analysed by Fellin [2002] and a brief study by Song et al. [2018], to the best of the Authors' knowledge. The former considered propagation of a compressive wave under a single cycle of loading and unloading and showed that a shock wave forms as a result of soil non-linearity in oedometer-like conditions. The latter study [Song et al., 2018] considered a semi-infinite column with a rectangular shock pulse with loading and unloading fronts, which interact with each other due to the unloading wave being faster and chasing the slower loading wave. However, the semi-infinite column was modelled with linearly hardening plasticity on loading and pure elasticity on unloading, thus not being representative of real soil behaviour. The importance of unloading waves in soil addressed in larger extent has been presented only recently [Kowalczyk, 2020]. This work showed for example how propagation of unloading waves in a semi-infinite column results in a weak strain discontinuity occurring in initially perfectly sinusoidal wave. Nevertheless, none of these studies identified potential release of soil elastic waves in relation to the propagation of unloading waves in hysteretic soil.

This paper suggests a potential explanation to the presence of high frequency motion in numerical and experimental studies as possibly related to the hypothetical, unknown before, physical phenomenon of soil elastic waves released and "trapped" due to reflections in a soil column modelled with a nonlinear hysteretic material. The presented study comprises primarily simplified numerical studies compared in chosen cases with experimental examples from the literature. In more detail, Section 2 of the paper is dedicated to methodology, including introduction to the conducted numerical studies and a short description of the experimental setups available to the Authors. Section 3 presents results of the numerical studies of a soil column of the height representative of a typical soil container in experimental setups. Mainly numerical consideration, supported where available by experimental data from the literature, is given to the hypothetical idea of the release of soil elastic waves. Primarily the dynamic response to harmonic excitation is analysed, but some consideration is given also to scaled earthquake input motion. Finally, a numerical study of a boundary value problem is compar ed with the available experimental data of a similar testing setup to reveal how the structural response of a pile may possibly be affected by the release of soil elastic waves. The discussion in Section 4 follows with further comments on the consequences of the potential existence of soil elastic waves in the dynamic response of soil, including their potential importance when understanding some observations in large magnitude earthquakes from the past. Finally, the most important findings are summarized in Section 5 with the conclusions of this paper.

2. Methodology

2.1. Numerical studies

The numerical studies in this paper are based primarily on analyses carried out by a simplified soil constitutive model. An advanced soil constitutive model, implemented in the multiaxial stress space, is used when comparing numerical results of a boundary value problem with a pile. The simplified 1D soil constitutive model, incorporating the basic ingredients of the advanced model, has been chosen to limit the constitutive features only to those sufficient to discuss the nature of the release and the "entrapment" of soil elastic waves in a soil column of a given height.

The numerical models include a simple geometry of a 0.8m high soil column representative of a typical soil specimen in small scale experimental works. The soil density has been set to 1332kg/m^3 unless specified otherwise. The boundary conditions allow full wave reflections at the base since soil containers are placed on rigid shaking tables. The side nodes of the soil column are linked by tie connectors ensuring the same lateral and vertical displacements of the nodes at the same height. The soil column has been discretized into 32 eight-node, quadratic finite elements of an equal size of 0.025m. This mesh refinement ensures that the element size is less than the standard "rule of thumb" and accounts for the refined mesh size criteria proposed by Watanabe et al. [2017]. In more detail, taking the highest frequency of interest to be 80Hz as per one of the reference experimental works [Durante, 2015], the slowest elastic shear wave velocity at shallow depth being approximately 40m/s, one obtains the maximum distance in grid spacing of 0.05m (i.e. the quadratic element size of 0.1m) for the standard discretization rules. Watanabe et al. [2017] showed that such grid spacing may need to be reduced to account for soil non-linearity and reduction in the shear wave velocity due to the developing plasticity. As such, the chosen quadratic element size of 0.025m can be considered much smaller than the standard discretization practise and within the updated discretization guidelines proposed by Watanabe et al. [2017].

The time increment in the numerical studies has been chosen to ensure the fastest shear wave in the soil column (i.e. around 120m/s at soil base) does not reach two consecutive nodes within the same time increment. As such, the time increment of $2{\cdot}10^{-5}$ second has been chosen for the advanced soil constitutive model implemented with an implicit integration scheme, and $1{\cdot}10^{-5}$ second for the simplified soil constitutive model, since the constitutive law is integrated with an explicit integration scheme.

The soil column in the numerical studies is subjected to horizontal acceleration time histories applied at base. The analysed input motions include primarily sinusoidal input motions (inspired by those typically applied in experimental works) and a case of scaled earthquake input motion. Perfectly sinusoidal input motions are introduced in a smooth manner, i.e. with the initial acceleration increment being very small, thus the initial displacement and velocity being practically nul.

2.1.1. Simplified constitutive model

This paper shows a simplified numerical study on the propagation of a sinusoidal wave in a soil column of 0.8m height. For this purpose, taking inspiration from the typical stress-strain response of soils, a simple 1D constitutive model based on a hyperbolic response and leading to nonlinear hysteretic behaviour was implemented as a user-defined subroutine (UMAT) of ABAQUS FEM code [Dassault Systèmes, 2019]. The column is modelled with a material of the following constitutive law:

$$\dot{\tau} = \begin{cases} \frac{(-\tau_{lim}(d)-\tau)^2}{2{\cdot}B{\cdot}\tau_{lim}(d)} \cdot \dot{\gamma}, \text{ for } \dot{\gamma} < 0 \\ \frac{(\tau_{lim}(d)-\tau)^2}{2{\cdot}B{\cdot}\tau_{lim}(d)} \cdot \dot{\gamma}, \text{ for } \dot{\gamma} > 0 \end{cases} \tag{1}$$

where B is the constitutive parameter defining the stiffness and:

$$\tau_{lim}(d) = \frac{\sqrt{d}}{\sqrt{d_{max}}} \cdot \tau_{lim} \tag{2}$$

where τ_{lim} is the limiting (positive) value of the stress, d is the current depth in the soil column, d_{max} is the maximum depth, i.e. in this work 0.8m. τ_{lim} and B are the model parameters chosen to be τ_{lim}=6000Pa and B=0.00016 unless stated otherwise. Note that the dependency of the stiffness and strength on a square root of depth can be deemed equivalent to the commonly assumed dependency on the stress level (which is also typically expressed as a square root). The model response can be imagined to be representative of the shear stress versus shear strain response in a simple shear test at small strain levels, in which the volumetric behaviour is not considered and the material hysteresis remains relatively narrow. In general, the simplified model can be deemed as approximately representative of any family of constitutive models in the finite element codes which predict a hysteretic type of stress-strain behaviour.

The simplified model has been calibrated to ensure in an approximate manner realistic representation of soil response in 1g small-scale experiments in flexible soil containers. To achieve this aim, similar approach has been adopted herein as for advanced soil constitutive models in the previous work [Kowalczyk, 2020]. The initial G_0 shear stiffness has been calibrated to reflect the G_0 shear stiffness evaluated from the empirical expression [Hardin and Drnevich, 1972] and the shear stiffness degradation G/G_0 has been fitted to the recommendations by Dietz and Muir Wood [2007] for simple shear deformation at low mean effective stresses, i.e. as relevant for 1g experimental setups subjected to horizontal shaking. Details of the calibration of the constitutive model (1) are shown in Appendix A. The stress-strain response of the model at two chosen depths is shown in Figure 1. The initial G_0 shear stiffness profile with the corresponding initial shear wave velocity profile predicted by the constitutive law (1) is shown in Figure 2. The fastest time of a wave travelling from the bottom to the top of the soil column for the given definition of the initial G_0 profile is approximately 0.0085sec (note that this time changes slightly when the hysteresis shape becomes wider). The first natural frequency of the soil column for an average shear wave velocity of 95m/s is slightly below 30Hz as evaluated from the well-known analytical expression: $f=v_s/4H$ (e.g. [Kramer, 1996]), where v_s is the average shear wave velocity, H is the height of a soil column. This assessment has been verified numerically as shown in Appendix B, where a slightly higher value of 33Hz has been indicated for the first natural frequency of the soil column when this has been subjected to an input motion of a flat frequency spectra (i.e. a white noise type of motion). In addition, the second soil natural frequency was evaluated to be around 88.5Hz as shown in Appendix B, which is close again to the value of 89Hz computed using the simple empirical approach. This evaluation of soil natural frequencies will be shown important when presenting the idea of the release of soil elastic waves.

Note that the Authors in this work preferred the simplified constitutive model for the sake of identifying the basic ingredients needed to observe the phenomenon of soil elastic waves in soil experiencing non-linearity. However, the general patterns of the shown results can be easily replicated when using other constitutive approaches provided those approaches account for soil inherent non-linearity in the form of a material hysteresis. For example, one can use the Severn-Trent sand model by Gajo [2010], a hypoplastic sand model by Von Wolffersdorff [1996] with the Intergranular Strain by Niemunis and Herle [1997] or one of the SANISAND models by Dafalias and Manzari [2004], as shown initially by Kowalczyk [2020].

2.1.2. Advanced soil constitutive model

An advanced elastoplastic soil constitutive model [Gajo, 2010] has been used in the numerical simulations of a small-scale experimental setup with a pile. Such constitutive model incorporates all the features of the simplified model, but in addition offers much more accurate representation of the real soil behaviour under cyclic loading in the multiaxial stress space. Short description of the elastoplastic model used herein is given below.

The elastoplastic sand model by Gajo [2010] is a classical kinematic hardening elastoplastic model. Its current model formulation is based on the former formulation by Gajo

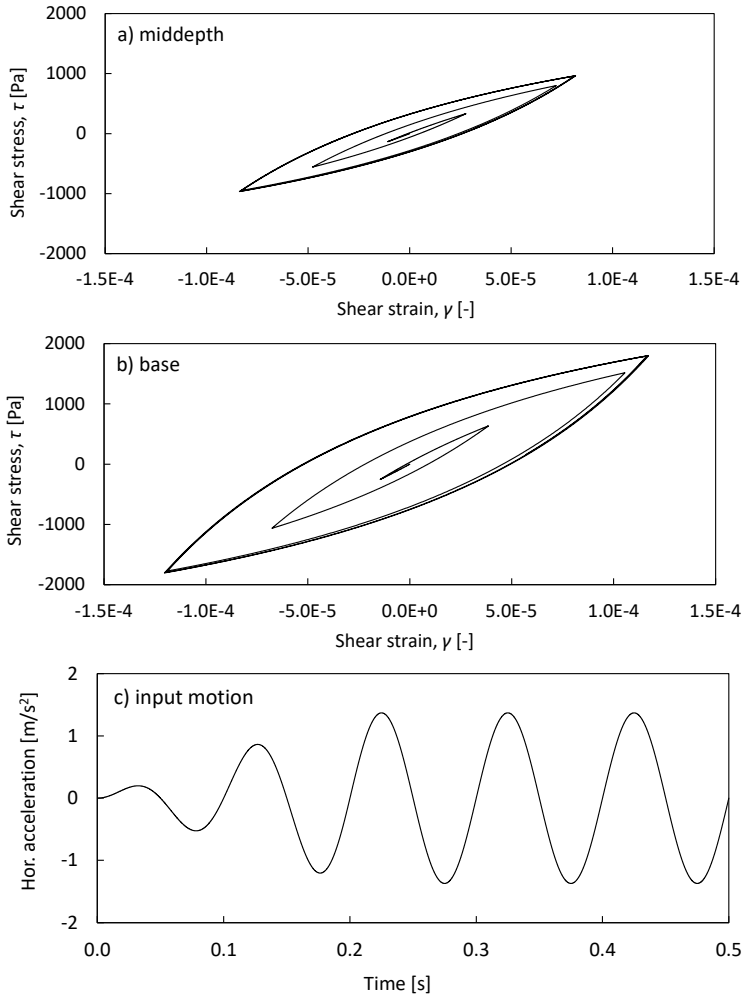

Figure 1. Response of the simplified 1D constitutive law (1): a) at mid-depth and b) at base of the 0.8m high soil column, c) under ramped up sinusoidal input motion applied at base.

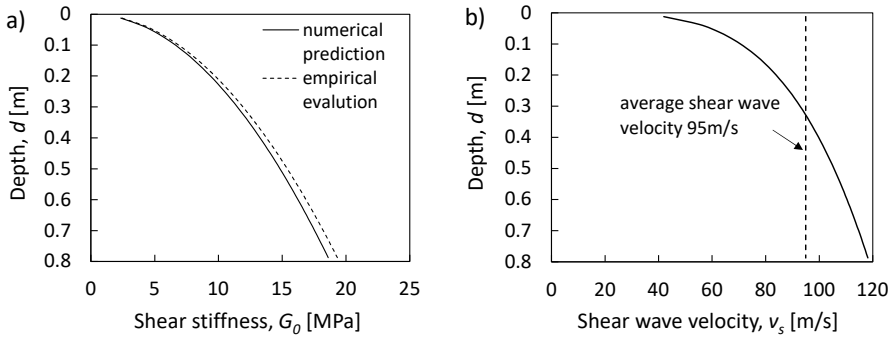

Figure 2. Stiffness characteristics of the soil column modelled with the constitutive law (1): a) the initial G_0 shear stiffness profile (compared with the empirical evaluation by Hardin and Drnevich [1972]) and b) the corresponding initial shear wave velocity profile.

and Muir Wood [1999a,b]. The model focuses on the deviatoric soil response, thus neglecting grain crushing under high pressures, and is based on the concepts of classical kinematic hardening to keep some memory of the past loading history. Importantly, the formulated model is based on the well-known concepts such as: the critical state, the Mohr-Coulomb failure, the state parameter Ψ [Been and Jefferies, 1985] to determine the dependence of the soil state on density and pressure, and plastic hyperbolic stiffness dependence on the distance from the failure surface. Further details of the model formulation are not presented herein for the sake of brevity and the interested Reader can find those in the cited works.

The calibration of the constitutive model is based on the general guidelines given by Dietz and Muir Wood [2007] for stiffness degradation expressed as G/G_0 for simple shear deformation in small scale experiments carried out in dry sand. These guidelines were supported by the limits identified by Seed and Idriss [1970] and the laboratory experimental data obtained by Kokusho [1980], both carried out on different sands, therefore can be deemed appropriate for sands in general. The model parameters are shown in Table C.1 and the calibration of the model is shown in Figure C.1 in Appendix C together with the validation of the calibration when simulating a cyclic simple shear laboratory test (Figure C.2).

2.2. Benchmark experimental work used in comparisons

Chosen numerical cases in this paper are compared with available experimental example tests on dry sand placed in a flexible soil container. A brief presentation of the reference experimental works is provided below.

The work by Durante [2015] was aimed primarily at investigating seismic soil-structure interaction of a group of five piles, however; free field measurements were also obtained. The soil container of 0.8m height was filled by using a pluviation method with two layers of Leighton Buzzard (LB) sand, the top "softer" layer of LB sand fraction E, the bottom "stiffer" layer of LB sand fractions B+E. The initial density of the top layer is 1332kg/m^3 and the void ratio of around 0.9, whereas for the bottom layer it is 1800kg/m^3 and 0.53, respectively. Nevertheless, note that the difference in terms of the relative density between the two soil layers is rather small (approximately 0.25 for the top layer, 0.4 for the bottom layer). Therefore, the numerical studies assume modelling a single homogeneous soil layer and can be deemed approximately representative for the experimental work of Durante [2015]. The experimental measurements were filtered with a low-pass filter of 80Hz, 5th order. The soil natural frequency was estimated to lie within the range of 25-30Hz depending on the amplitude of the input motion varying from 0.01g to 0.1g. The applied sinusoidal input motions considered various input frequencies and moderate amplitudes of up to around 0.15g. More details on the experimental work can be found in the experimental research works [Durante, 2015], [Durante et al., 2016].

The experimental work by Dar [1993] was carried out in a flexible soil container of 0.8m height, i.e the same height as the experimental work of Durante [2015]. The main difference with respect to the experiments by Durante [2015] is that the soil container was filled with a single homogeneous soil layer of LB sand, fraction B. The achieved void ratio was evaluated to be around 0.6 resulting in the relative density of 0.75, i.e. as per dense sand. The density of the deposited sand was around 1700kg/m^3. The experimental measurements included free field response as well as investigation of soil-structure interaction. The natural frequency of the soil was evaluated by Dar [1993] to be around 23Hz, for the amplitude of motion of 0.1g. The amplitudes of the applied sinusoidal input motions included strong motions as large as 1.0g.

Table 2.1. Summary of the input parameters of the constitutive model (1) to model different experimental setups

Experimental setup	τ_{lim}	B	d_{max}
Durante (2015)	6000	0.00016	0.8
Dar (1993)	15000	0.0002	0.8

Note that to account for denser sand used by Dar [1993], the calibration of the constitutive model (1) has been revised when compared to the main calibration discussed in Section 2.1.1. Details of the revised calibration for this case are provided in Appendix A. The input parameters used in the numerical studies to account for both experimental setups are summarized in Table 2.1.

3. Results

Comparison of linear elastic soil with hysteretic soil

Firstly, the soil column is modelled with linear elastic properties equivalent to the shear stiffness profile shown in Figure 2a (i.e. depth dependent stiffness) without any addition of damping in the system. This short study is to show the dynamic response of the linear elastic column to harmonic excitation and subsequently, how this response differs from the response computed for the soil modelled with a hysteretic material.

The linear elastic soil column having the first natural frequency of 33Hz is subjected to 10Hz input motion. For the smoothly introduced input motion (Figure 3a), the response at the top of the column is slightly affected by an additional wave which can be identified as an elastic wave in the spectral response (Figure 3c). Note that the elastic wave affecting the motion at the top of the column does not produce repetitive sine cycles (i.e. the consecutive sine cycles of the motion slightly differ from each other). Since no damping is present in the model and the base is rigid, the released wave remained "trapped" in the column during the constant amplitude part of the input motion and after the driving force is ceased. On the other hand, when the motion is introduced in an abrupt manner (Figure 3b), the computed response at the top of the column appears to be heavily affected by additional waves due to, what could typically be considered, the transient response to the abruptly introduced force. In fact, after the driving force is steadily ramped down to nul (in the same gradual manner as per the smoothly introduced motion), the presence of the elastic wave is characterised by large amplitude and an increased amount of higher natural frequency components. This is confirmed by investigating the evaluated spectral response for both cases, when the harmonic driving force is applied, and when it is ceased in the coda part of the motion (Figure 3c and 3d, respectively). Note that the identified frequencies of 33Hz, 88Hz, 143Hz and 197Hz correspond to the natural frequencies of the soil column.

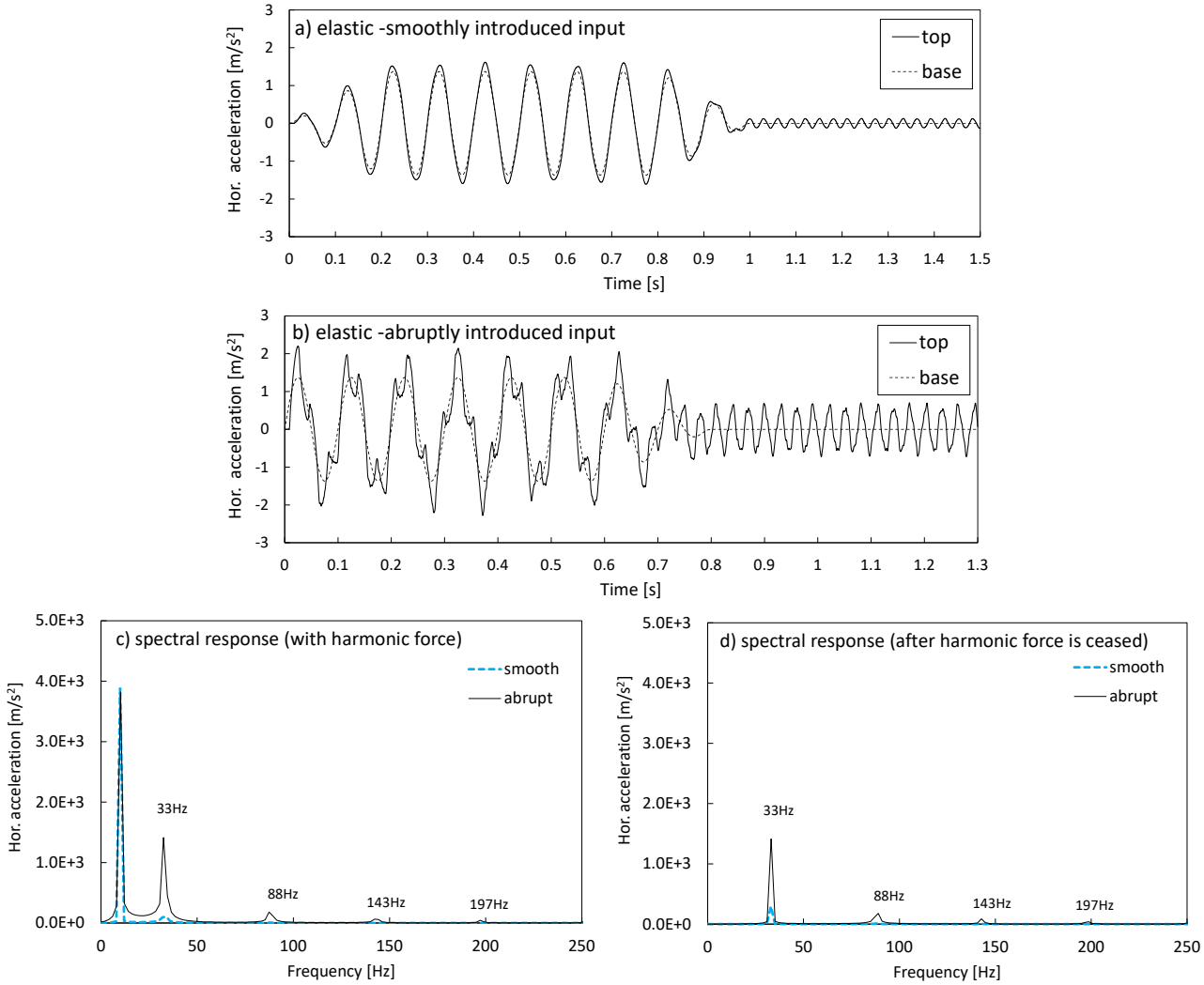

Figure 3. Horizontal accelerations computed for the 0.8m high soil column modelled with a linear elastic depth dependent material under harmonic (10Hz) input motion: a) response for smoothly introduced input motion, b) response for abruptly introduced input motion, c) evaluated spectral response while the harmonic force is being applied, d) evaluated spectral response in the coda part of the motion with the harmonic force ceased.

Nextly, the soil column is analysed under the same input motions but with a hysteretic material (1) with the G_0 initial shear stiffness as shown in Figure 2a. Note that in Figure 4 the amplitude of the input motion (0.137g) is such that the hysteresis loop is relatively narrow (i.e. little non-linearity develops), thus the constitutive model (1) remains fairly comparable with the linear elastic material used for the computations shown in Figure 3.

Figure 4a presents results for the smoothly introduced input motion. The response at the top of the soil column is not strongly affected by high frequency motion similarly to the case shown in Figure 3a. The computed amplitudes are very similar for both cases (Figures 3a and 4a), although the actual amplification of motion is slightly higher when using the nonlinear model compared with the linear elastic model (however, the very first cycle of the response, for which the nonlinear model remains practically almost linear, the amplification appears to be the same for both). The very beginning of the motion is in fact similar to the one computed in Figure 3a. However, later the material hysteretic damping appears ineffective in removing the high frequency motion. This high frequency motion appears from around 0.3sec in the consecutive sine cycles with the same repetitive pattern, i.e. a sort of "steady state" is apparently reached under the constant amplitude of the harmonic input motion. When the driving force is ceased, the high frequency waves are still present, however, in this situation the material damping appears sufficient to slowly reduce the amplitude of the remaining waves. Figure 4b shows the case of the input motion introduced in an abrupt manner. Again, the very first cycle of motion is comparable with this predicted by the elastic material (Figure 3b), with strong presence of high frequency motion. Nevertheless, this time this high frequency motion diminishes slightly in the consecutive sine cycles, such as this time the material hysteretic damping in the soil column is sufficiently effective. After a couple of cycles, again an apparent "steady state" emerges with no further damping out of the high frequency waves. The computed

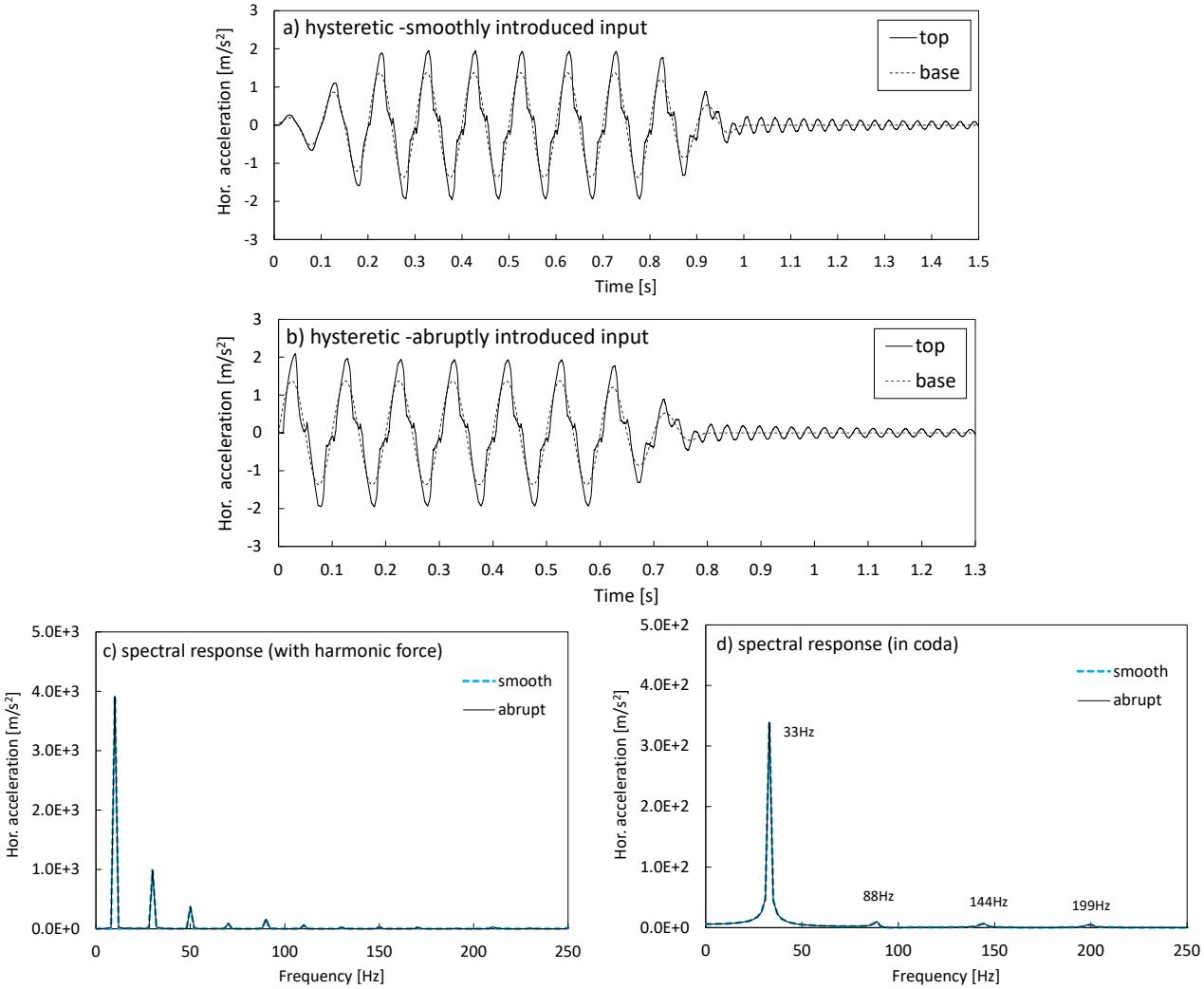

Figure 4. Horizontal accelerations computed for the 0.8m high soil column modelled with the hysteretic depth dependent material (1) under harmonic (10Hz) input motion: a) response for smoothly introduced input motion, b) response for abruptly introduced input motion, c) evaluated spectral response in the "steady state" (with the driving force), d) evaluated spectral response in the coda part of the motion (without the driving force).

"steady state" solutions for both cases (Figures 4a and 4b) appear to be exactly the same thus independent on whether the input motion is introduced smoothly (Figure 4a) or abruptly (Figure 4b). Consequently, so is the coda part of the motion after the driving force is ceased.

The spectral evaluation of the computed responses is shown in Figures 4c and 4d and confirms that the responses when the driving force is applied or ceased, in fact, perfectly match for both, smoothly and abruptly, introduced input motions. Note that the spectral response in Figure 4c has been computed when the sort of "steady state" has been reached, i.e. the response is characterised by repetitive sine cycles of the harmonic pattern of ω, 3ω, 5ω (where ω is the driving frequency). Moreover, the coda part of the motion reveals that the remaining waves in the system appear to be the soil elastic waves, i.e. soil natural frequencies of 33Hz and 88Hz have been identified, with frequencies of 144Hz and 199Hz being approximately representative of higher soil natural frequencies (see Figures 3c and 4d for comparisons). These elastic waves appear as "trapped" in the soil due to reflections from the top free end and the base fixed end, and are slowly being damped out due to hysteretic material damping.

The dynamic response of the soil column modelled with a hysteretic model is subject to further investigation when looking at loading cases representative of those typically experienced in flexible soil containers where the evaluated spectral responses are characterised by regular patterns of ω, 3ω, 5ω etc. To this aim, horizontal acceleration input motions of different driving frequencies and amplitudes are used in order to present how soil elastic waves can hypothetically be released in hysteretic nonlinear soil representing dry sand placed in a flexible soil container.

10Hz input motion, maximum amplitude of 0.03g

The first analyzed case shows the response of the soil column to the input motion of a relatively low amplitude (herein 0.03g) when the soil column behaviour would be expected to be very close to that of the linear elastic column.

It can be observed in Figure 5 that, in fact, the response of the top of the column is only slightly affected by the high frequency motion. Note that the spectral response evaluated from the response in the time interval 0.3-0.8sec (Figure 5c) reveals some very slight presence of the exact harmonic of 33Hz introduced as per the studies shown in the linear elastic column and left due to little damping, thus this time not fully representative of the "steady state"-like response. The almost linear response in the soil column and little damping are evident when investigating the stress-strain behaviour shown in Figure 6 with only some non-linearity developing at base. Note that the hysteresis at the top (plotted at the middle of the top element, thus slightly below of the actual top of the soil column), as well as the reached strain levels, is much smaller than the hysteresis and the strain levels at base. This is due to the boundary condition of zero stress and strain holding at the free end of the soil column and justifies why the stress strain response at the top appears to be almost linear.

10Hz input motion, maximum amplitude of 0.137g

Subsequently, the amplitude of the input motion is increased to 0.137g. Figure 7 reveals clear distortion of the sinusoidal wave, both in terms of the computed accelerations (Figure 7a) as well as the computed shear strains (Figure 7b). High frequency components of motion can be seen in the spectral response in Figure 7c. Importantly, the harmonic of 30Hz (i.e. close to the soil first natural frequency) has a large amplitude, moreover, the harmonic of 90Hz (i.e. close to the second natural frequency of soil) is also significant. Note that the remaining harmonics would be representative of the distortion of a sinusoidal wave towards a square wave as shown by others (e.g. [Pavlenko, 2001], [Mercado et al., 2018]). On the other hand, the high harmonics in Figure 7c are not of the exponential decay pattern (e.g. herein the harmonic 90Hz is of larger amount than the harmonic 70Hz), thus the evaluated pattern of high harmonics cannot be representative solely of the distortion towards a square wave but apparently could possibly be associated to the presence of soil elastic waves. The pattern of high harmonics in the evaluated response spectra is again in the form of ω, 3ω, 5ω etc. and represents the "steady state" when the computed consecutive cycles of response are the same. Thus, the exact values of soil natural frequencies (i.e. 33Hz and 88Hz) cannot be shown here. Figure 7d shows that the presence of high frequency waves is also visible in the computed relative displacements of the top to the base of the soil column. The hysteretic non-linearity in soil is shown in Figure 8 and confirms the observation from the previous analysed case that the hysteresis at the top is much smaller than at the base.

Finally, Figure 9 compares the computed accelerations at depth of about 40mm (filtered with a 80Hz Butterworth filter as per the experimental measurements) with the available experimental data [Durante, 2015] for the same input motion of 10Hz driving frequency and the amplitude of 0.137g. It can be observed that the amplitude of the motion has been captured correctly together with only little phase shift between the motion at the base and the top (as expected for the case of the driving frequency below the first soil natural frequency). High frequency motion is present in both; however, it is apparently more obvious in the computations, possibly due to different damping characteristics in the experimental setup. For example, damping induced by the physical presence of the soil container and the restraint metal frame around the soil container have not been modelled numerically but may play a role with this respect. Note that after the driving force was ceased, the experimental measurements at base were affected by high frequency recordings induced by the electric current and not representative of the actual motion applied to the experimental specimen. For this reason, this high frequency has not been included in the numerical model. Moreover, the experimental records experience non-symmetric response within a single sine cycle with stronger distortion observed on the downward branch of the measurements. This is possibly due to the accumulation of the plastic shear strains from the previous loading scenarios, not accounted for in the simplified numerical studies. Nevertheless, traces of regular patterns of high frequency motion are obvious in both, numerical and experimental results.

10Hz input motion, maximum amplitude of 0.2g

Figure 10 shows the results for 10Hz input motion with the amplitude of motion increased to 0.2g. Such amplitude results in more clearly visible high frequency motion, i.e. distortions in the computed accelerations (Figure 10a) and shear strains (Figure 10b), and the presence of high harmonics again not representative of the exponential decay pattern (see increased amounts of frequencies 90Hz, and 130Hz in Figure 10c). In case of the stronger amplitude of motion, further observation can be made regarding the release of soil elastic waves, i.e. the occurrence of strong discontinuity can be noticed in the computed strains. The occurrence of such strain discontinuity is shown in more detail on the enlarged view in Figure 11. Although very high frequency numerical oscillations (due to the problems of standard numerical algorithms in the finite element method to represent strain discontinuity) appear in the computed accelerations (Figure 11a) and shear strains (Figure 11b), regular "jumps" in these quantities can also be observed. It can be noticed that the time distance between these "jumps" at the soil column top is approximately equal to the time of 0.018sec needed for the fastest wave to travel from the top to the base, and reflecting back to the top. Note that following such reflection at base the shear strain moving upwards changes sign due to the phase change upon the reflection from the fixed end. The amount of the induced non-linearity for 10Hz 0.2g input motion shown in Figure 12 is higher than shown for the case of 10Hz 0.137g (see Figure 8 for direct comparison). Note that the increased amplitude of the reflected elastic wave is such that it causes unloading-reloading loops in the stress-strain response of soil at the top of the column (highlighted with a dotted circle in Figure 12a and shown in "zoom in" view in Figure 12c).

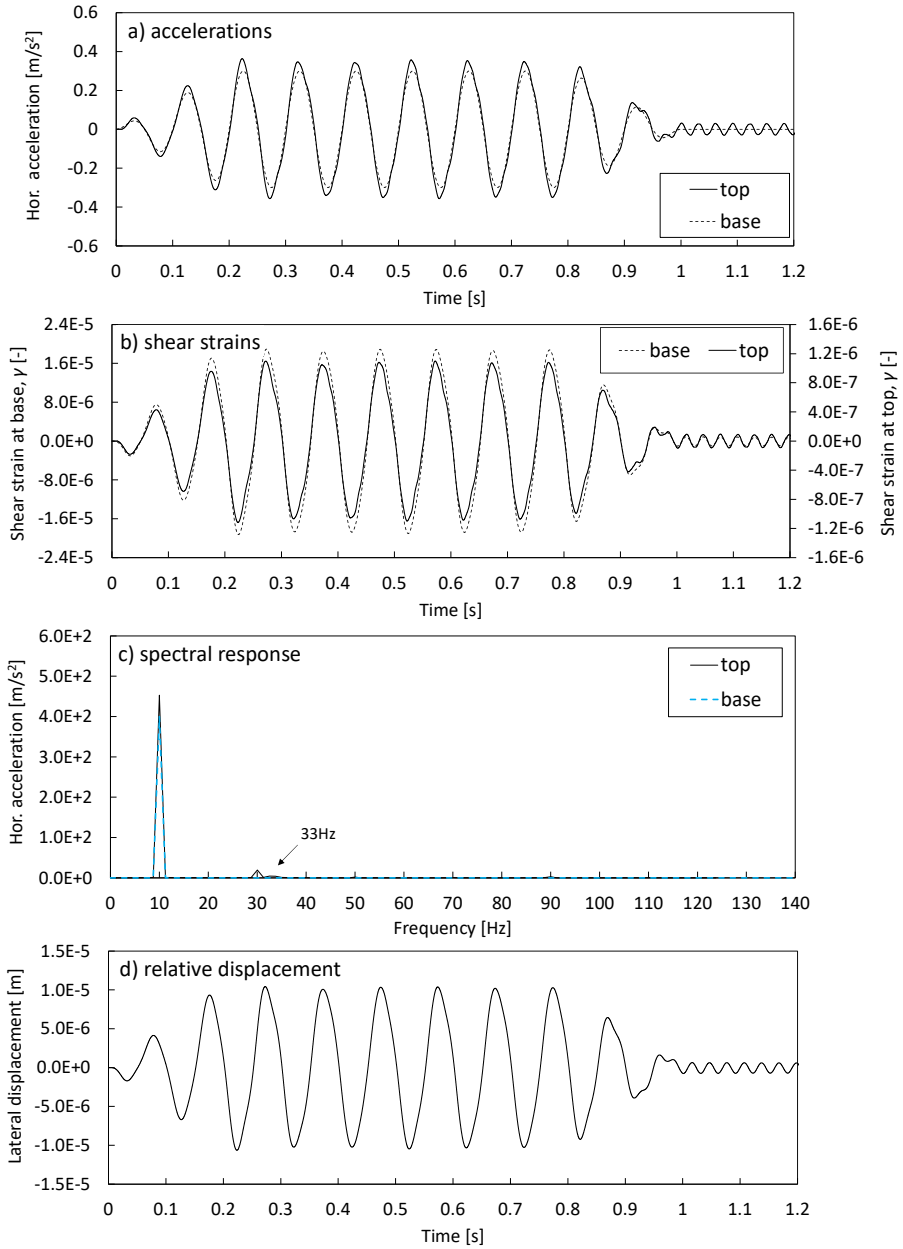

Figure 5. Computations for the soil column subjected to 10Hz input motion of the maximum amplitude of 0.03g: a) horizontal accelerations, b) shear strains, c) spectral response evaluated for the time window with the input motion of a constant amplitude, d) relative displacements.

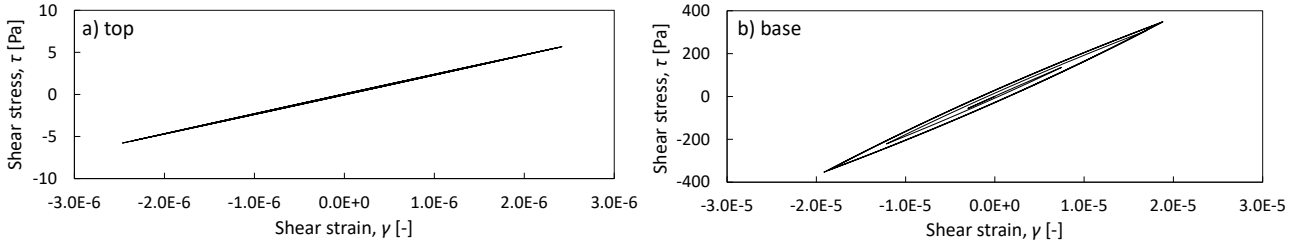

Figure 6. Computed stress strain curves for the soil column subjected to 10Hz input motion of the maximum amplitude of 0.03g: a) top of the soil column, b) base of the soil column (results shown up to 0.5s of the computed time history).

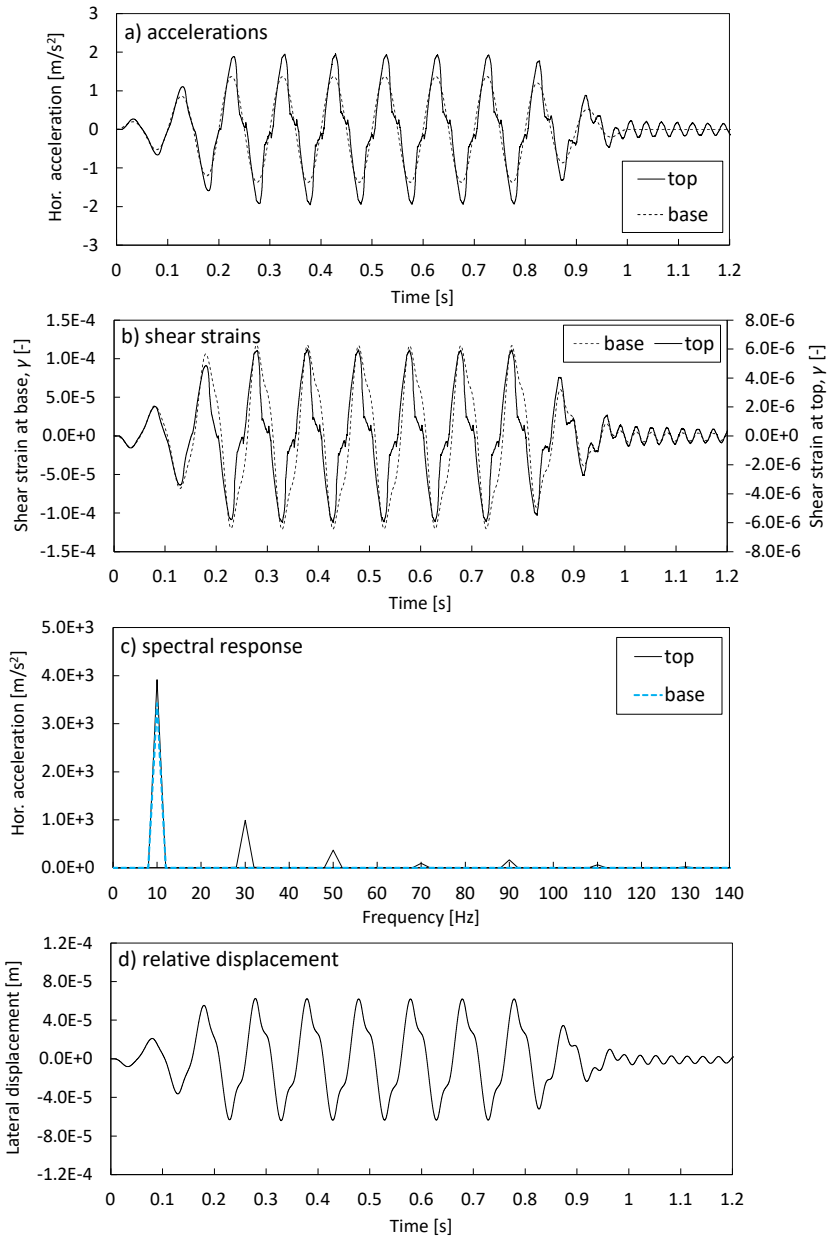

Figure 7. Computations for the soil column subjected to 10Hz input motion of the maximum amplitude of 0.137g: a) horizontal accelerations, b) shear strains, c) spectral response evaluated for the time window with the input motion of a constant amplitude, d) relative displacements.

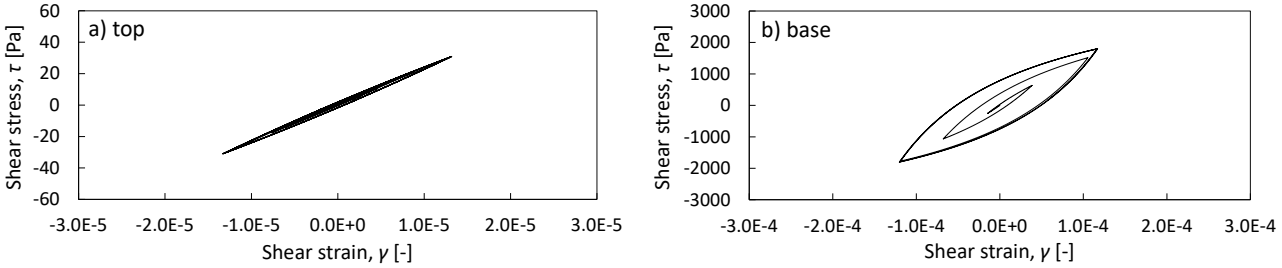

Figure 8. Computed stress strain curves for the soil column subjected to 10Hz input motion of the maximum amplitude of 0.137g: a) top of the soil column, b) base of the soil column (results shown up to 0.5s of the computed time history).

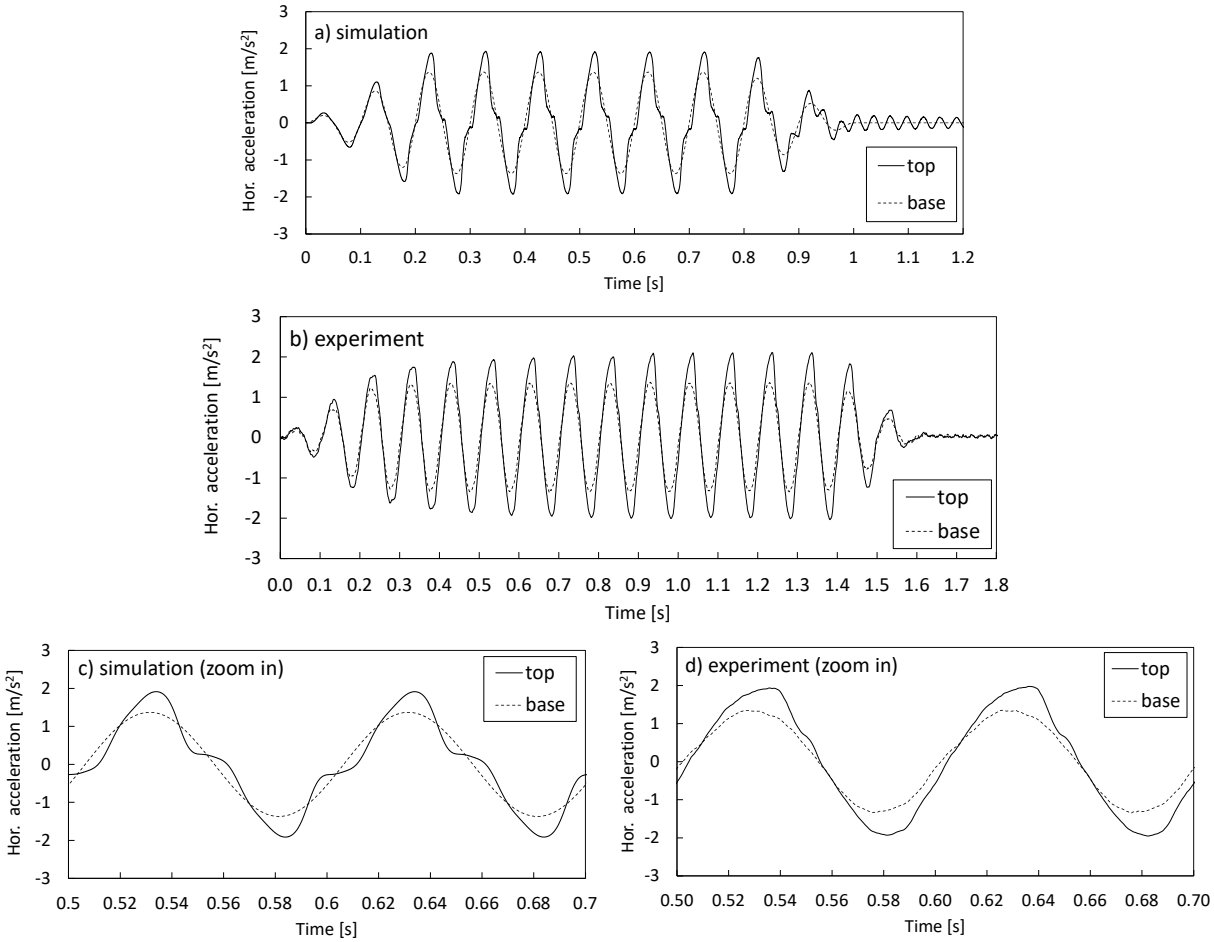

Figure 9. Comparison of filtered horizontal accelerations at depth of 40mm of the soil column subjected to 10Hz input motion of the maximum amplitude of 0.137g: a) numerical computations, b) experimental measurement data, c) numerical computations (zoom in), d) experimental measurement data (zoom in).

10Hz input motion, maximum amplitude of 0.63g

Figure 13 shows the computed accelerations when the soil column is subjected to even higher amplitude of input motion of 0.63g. The computations here are for a different experimental setup [Dar, 1993] in which denser sand was used. To account for this, the calibration of the constitutive model (1) has been revised as presented in Table 2.1 and Appendix A. The soil density has been set to 1700kg/m^3 as per the experimental assumptions. The comparison between the computations and the measurements indicates generally satisfactory agreement in terms of the amplitude and the presence of high frequency motion in the "steady state"-like response. Both, the simulations and experiments, have been heavily affected by repetitive high frequency motion. The patterns of responses are not fully consistent with each other; however, the observed high frequency motions are obtained for input motions of a single driving frequency (i.e. perfectly sinusoidal in the numerical study, and, from visual inspection, apparently perfectly sinusoidal also in the experiment [Dar, 1993]).

25Hz input motion, maximum amplitude of 0.077g

The next analysed case deals with the input motion of a driving frequency of 25Hz and the maximum amplitude of 0.077g. As shown in the computed accelerations and shear strains on Figures 14a and 14b, respectively, a "jump" in the accelerations occurs due to the discontinuity in strains (thus also the occurrence of very high frequency numerical oscillations). Apparently for higher frequency of the input motion (25Hz) even a lower amplitude than for the 10Hz input motion (i.e. Figure 10) is enough to observe a strong strain discontinuity. On the other hand, this time the released elastic wave travelling towards the base of the column does not return back to the top of the column in the "steady state"-like cycles. This can be seen in the computed accelerations and shear strains but also in the relative displacements (the latter one is this time in a form of a single frequency for the time period with the harmonic force applied). The evaluated spectral response of the horizontal accelerations computed at the top (Figure 14c) shows high harmonics; however, these are due to the representation of the "jumps" in the accelerations and not the reflections of the elastic waves. For this reason the consecutive harmonics occur with the exponential decay in

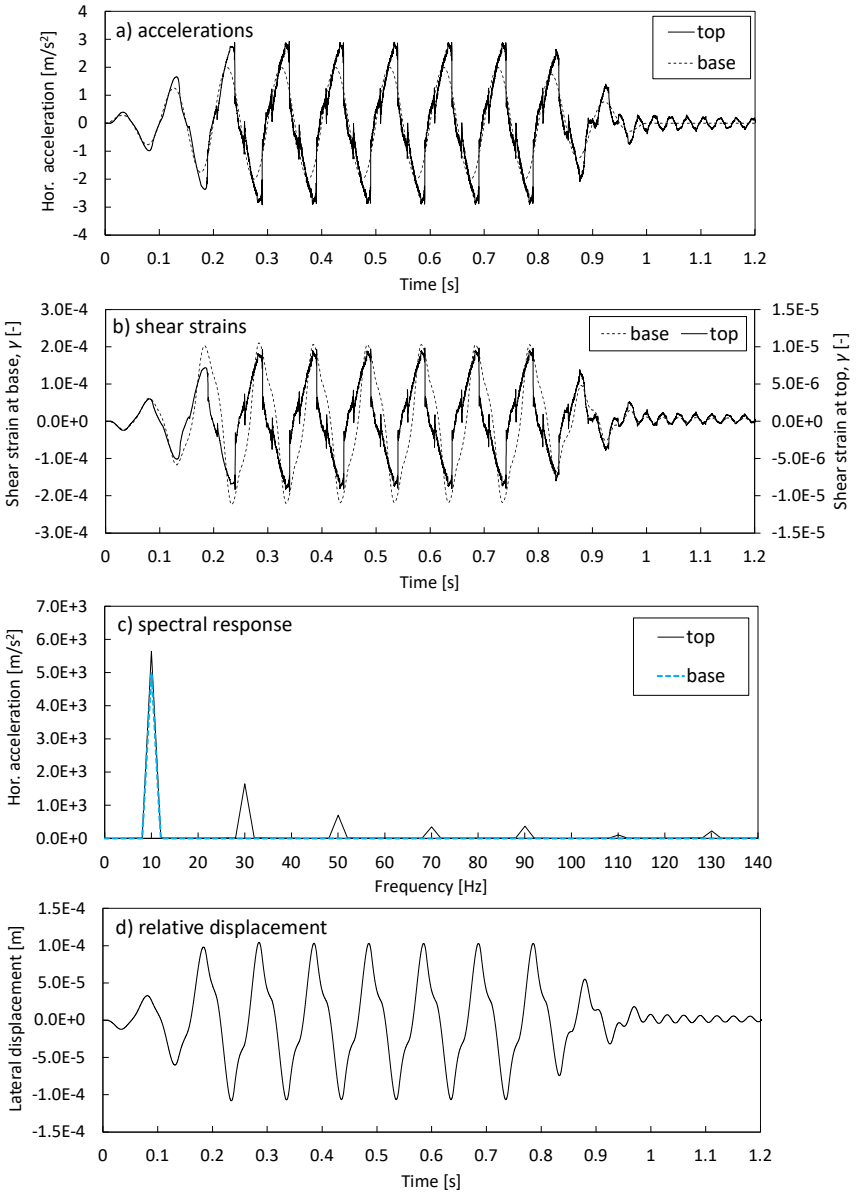

Figure 10. Computations for the soil column subjected to 10Hz input motion of the maximum amplitude of 0.2g: a) horizontal accelerations, b) shear strains, c) spectral response evaluated for the time window of the input motion of a constant amplitude, d) relative displacements.

their amounts. The presence of the reflections of soil elastic waves is more explicitly revealed only in the coda part of the motion when the driving force is ceased. For example, the period of the relative lateral displacements changes from 0.04sec to 0.03sec (i.e. representative of an elastic wave of around 33Hz frequency). The observation that the response under harmonic excitation at the column top is not affected in this case by the wave reflection is due to the fact that the time required by the elastic waves to travel down and up again is longer than the subsequent unloading taking place at the base of the column. This is the consequence of inducing motion with higher frequency of 25Hz rather than 10Hz. Finally, Figure 15 compares the filtered computed accelerations with the recorded ones [Durante, 2015]. Generally, the amplitude of motion is similar as is the phase shift with some difference observed in the form of distortion of the sinusoidal wave.

Scaled real earthquake input motion

To complement the use of simplified sinusoidal input motions where the identification of soil elastic waves might be easier, the Authors present also a case of earthquake input motion. The chosen transient loading history is a scaled Tolmezzo earthquake as analysed by Durante [2015]. The analysed herein duration includes the first 1.5sec of the time history. The computed and measured time histories are shown in Figures 16a and 16b. The experimental acceleration data is available only in a filtered format, thus, it is not possible to clarify if the generated high frequencies are representative of soil elastic waves. On the other hand, the computed accelerations can represent in certain parts

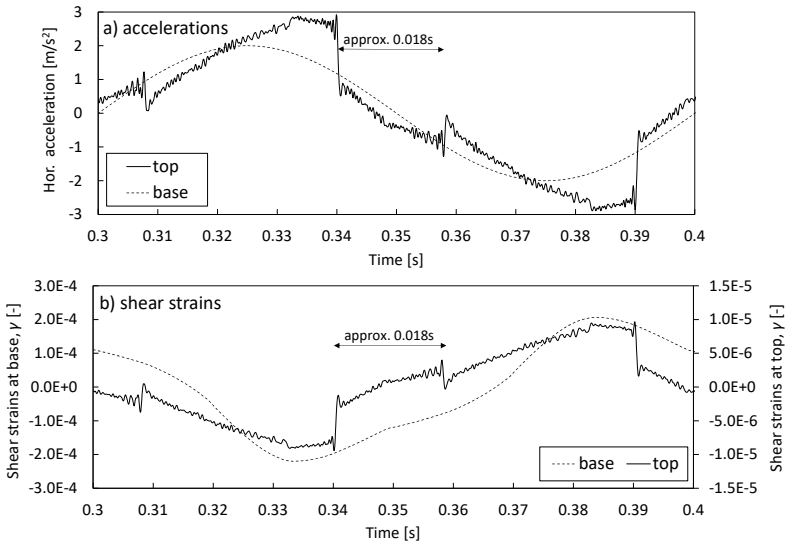

Figure 11. Computations for the soil column subjected to 10Hz input motion of the maximum amplitude of 0.2g in the time period between 0.3-0.4sec: a) horizontal accelerations, b) shear strains.

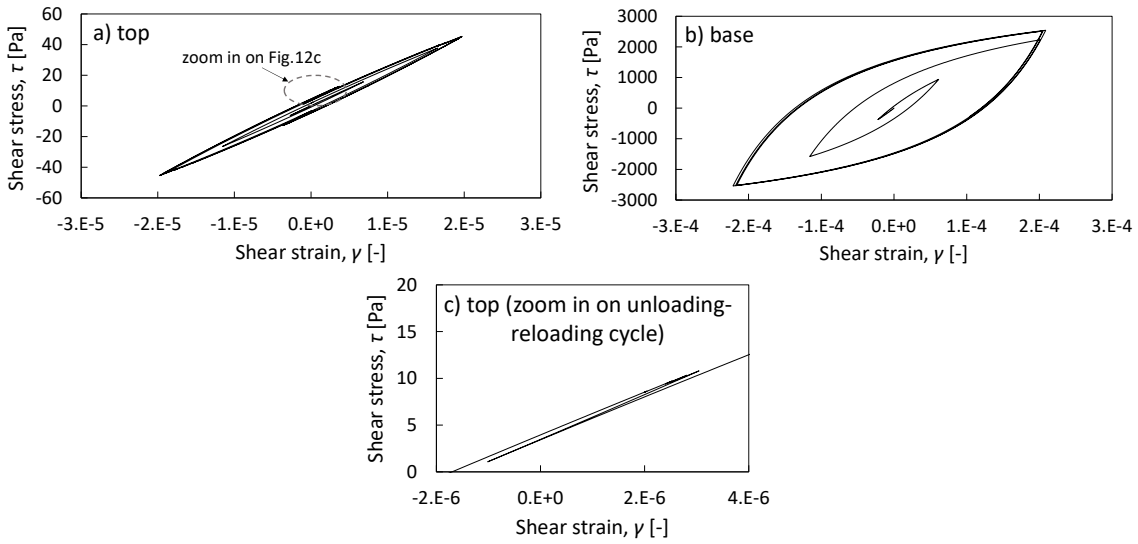

Figure 12. Computed stress strain curves (plotted up to 0.5s of the computed time history) for the soil column subjected to 10Hz input motion of the maximum amplitude of 0.2g: a) top of the soil column, b) base of the soil column, c) zoom in on the unloading-reloading strain cycle at the top of the soil column at approximately 0.36s (compare with the shear strain profile in Figure 11b).

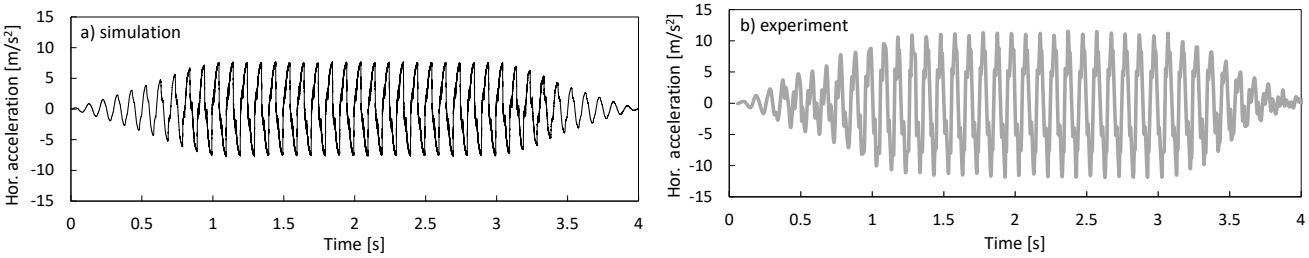

Figure 13. Comparison of horizontal accelerations at depth of around 100mm of the soil column subjected to 10Hz input motion of the maximum amplitude of 0.63g: a) computations, b) experimental measurement data digitized from [Dar, 1993].

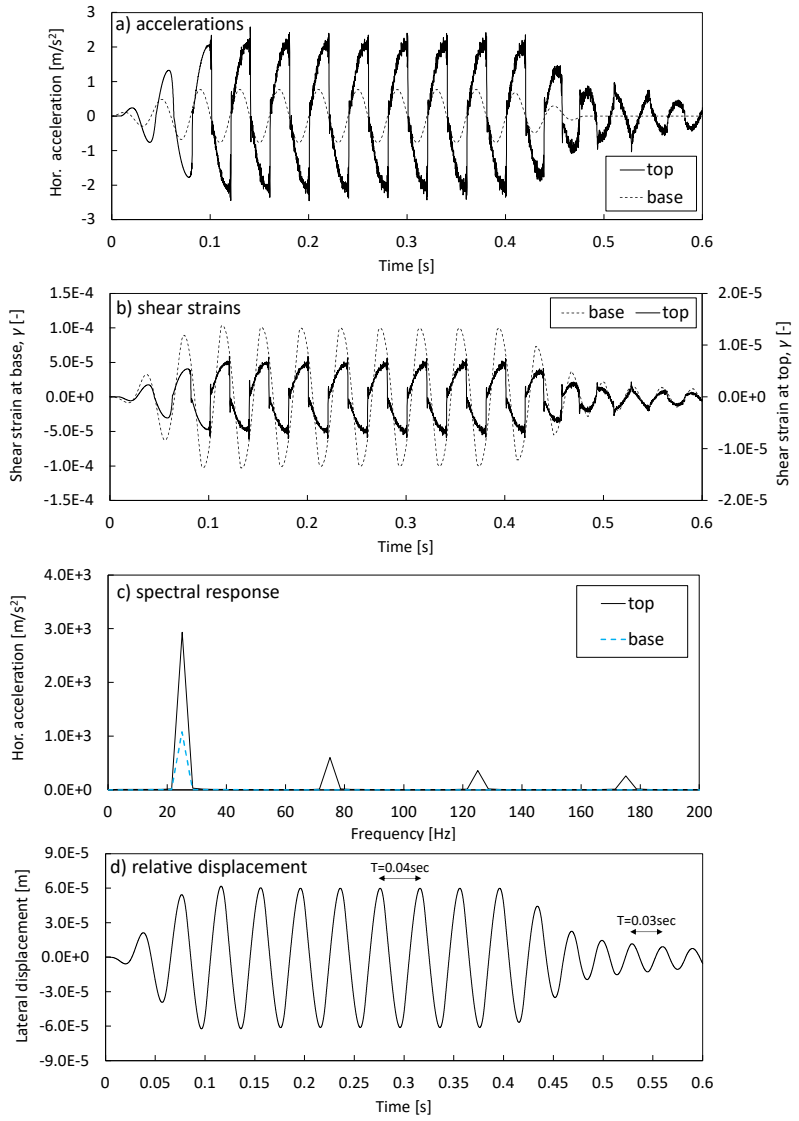

Figure 14. Computations for the soil column subjected to 25Hz input motion of the maximum amplitude of 0.077g: a) horizontal accelerations, b) shear strains, c) spectral response evaluated for the time window with the input motion of a constant amplitude, d) relative displacements.

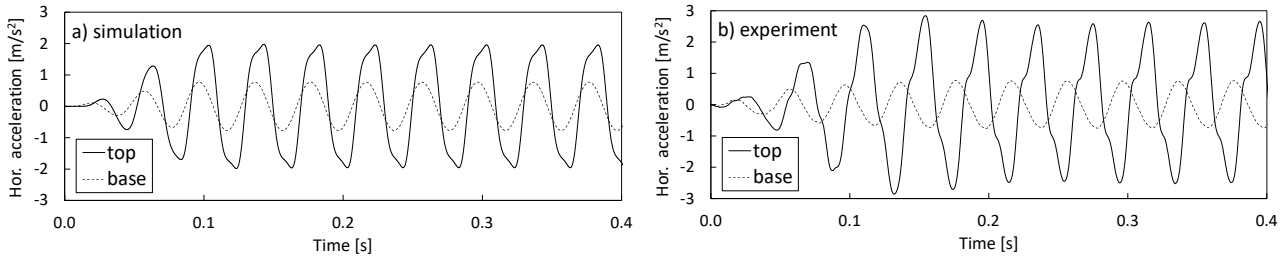

Figure 15. Comparison of filtered horizontal accelerations at depth of 40mm of the soil column subjected to 25Hz input motion of the maximum amplitude of 0.077g: a) simulation, b) experimental data.

of the motion (i.e. when the incident motion is of a lower frequency and amplitude) the presence of soil elastic waves "trapped" in the soil column as indicated in Figure 16c for the motion between 0.5-0.7sec. For completeness, the detail of the time history between 0.5-0.7sec is also shown for the experimental measurements (Figure 16d). Here one may also find patterns of the response resembling those potentially representative of soil elastic waves. Finally, the evaluated spectral responses at the top of the soil column (Figures 16e and 16f) confirm the presence of some high frequency components of motion even though these were absent at the base level. Note that the analysed case of the

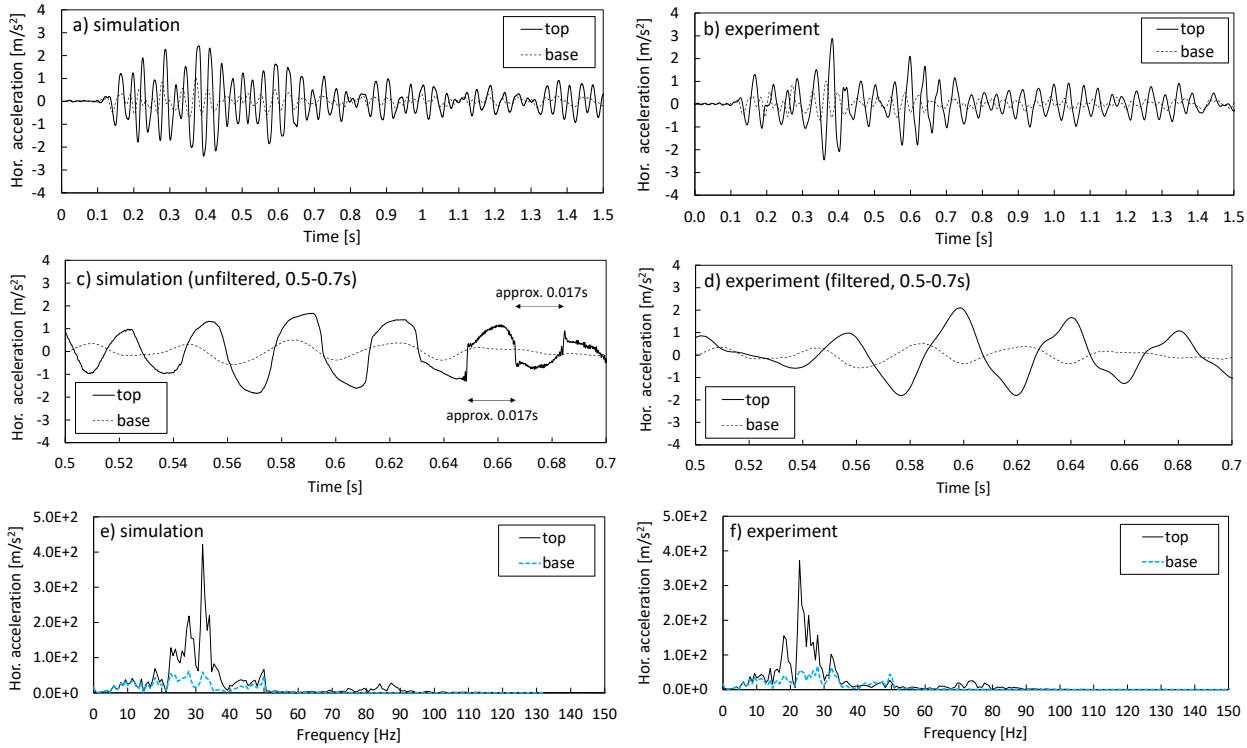

Figure 16. Comparison of the horizontal accelerations of the soil column subjected to the scaled earthquake input motion: a) numerical computations (filtered), b) experimental data (filtered), c) numerical computations between 0.5-0.7s (unfiltered), d) experimental data between 0.5-0.7s (filtered), e) evaluated spectral response for computations, f) evaluated spectral response for experimental measurements.

scaled earthquake does not present any longer the "steady state"-like response as per the previously analysed cases with harmonic excitation. Nevertheless, it reveals how soil elastic waves may potentially be also released in real earthquakes and remain "trapped" in a stratum if a rigid or much stiffer formation constrains this stratum at base.

Short summary of free field numerical studies

To sum up, the results of the free field response have revealed how high frequency motion in the computations can possibly be representative of an unrecognized before hypothetical phenomenon of soil elastic waves released due to soil inherent non-linearity in a form of material hysteresis. This phenomenon has been shown to manifest itself through reflections of the elastic waves inside a soil column and the occurrence of strong strain discontinuity in the computed strains, both leading to the observation of high frequency components.

The reflections of soil elastic waves have been easier to be identified in the computations for input frequencies below the first soil natural frequency (i.e. 10Hz herein) and in low-frequency part of the scaled earthquake loading. In such case, the "entrapment" of soil elastic waves in the soil column can be clearly observed in the computed accelerations, shear strains and relative displacements at the top of the column. In fact, one could analyse a case with input motion of an even lower driving frequency than 10Hz, which would allow for an increased number of elastic wave reflections in the soil column (omitted here for the sake of consistency with typical input motions applied in experimental works). On the other hand, for the input frequency of 25Hz (i.e. close to the soil natural frequency) the observation of the reflected elastic waves is clear only in the coda part of the motion in the computed accelerations and relative displacements. The second manifestation of the presence of soil elastic waves is the occurrence of strong strain discontinuity in the computed strains as observed for the input motions of increased amplitude (case of 10Hz, 0.2g) or the driving frequency close to the first natural frequency of soil (case of 25Hz, 0.077g).

The amplitude of the released elastic waves has been shown to be related to the amount of non-linearity developing in soil, i.e. increased changes from loading to unloading/reloading stiffnesses (in other words thickness of hysteresis). Thus, higher amplitude of input motion results in higher amplitude of the released elastic waves (see Figures 5, 7 and 10 for comparison of 10Hz input motions of increasing amplitudes).

Note that it has not been explicitly shown when in the loading cycle, or where in the soil column the elastic waves are released. It can be speculated that this is at the base when the sudden changes in stiffness (i.e. from loading to unloading) take place on load reversals or, alternatively, at the top when incoming waves are reflected from the free end. Certainly, future studies could address this aspect in more detail, for example when employing a finite element algorithm less affected by very high frequency numerical oscillations.

Boundary value problem of soil-structure interaction

Finally, this section presents a comparison of the numerical and experimental results for a boundary value problem on an example case of dynamic soil-structure interaction. It reveals how soil generated high frequency motion, possibly representative of soil elastic waves, can impact on structural response. In this case, a slender pile embedded in soil and with a small mass attached to its top (as a result of the attached fixing and measuring devices) is subject to a simple analysis.

The soil and pile discretization is shown in Figure 17. Only a half of the flexible soil container has been modelled in order to reduce the computational times. The soil has been modelled with an advanced elastoplastic soil constitutive model [Gajo, 2010] and assuming homogeneous soil, similarly to the studies in free field. The soil element size for the full 3D analysis has been optimised for the sake of the computational time. Instead of 32 equal size elements of 0.025m along the 0.8m height (as in the free field studies), herein 22 quadratic brick elements have been used. However, the element size has been varied from 0.02m at the top to 0.06m at the bottom, therefore, accounting for slower waves propagating in soil at the top of the soil container. The chosen range of element size remains well within the standard meshing procedures as explained in Section 2.1.

The boundary conditions have been specified at the soil side and base nodes. The base nodes were constrained in the vertical direction with a horizontal acceleration time history being applied. The long soil side nodes have been constrained in the horizontal direction perpendicular to the long side plane. Finally, the corresponding nodes on both short sides have been tied together to ensure the same horizontal displacements on both sides to mimic the presence of the lateral constraint provided by the flexible soil container.

Note that the 3D numerical study accounts for the presence of a single pile only, whereas the experimental setup of Durante [2015], to which the numerical results are compared, contained five piles. The reason for modelling a single pile only is to show to the Reader that the computed oscillations in the accelerations of the pile can be related only to the high frequency motion generated in soil and not to the interaction between the piles. Nevertheless, previous numerical studies [Kowalczyk, 2020] showed that the same patterns of response can also be observed if the whole group of five piles is modelled or if a different seismic input motion is analysed.

Figure 18 shows the comparison of the computed and measured horizontal accelerations on piles when soil specimen is subjected to 10Hz input motion of 0.137g. It can be observed that the high frequency oscillation motion is present in both, the computations and the experiments [Durante, 2015]. The high frequency motion is in the form of a regular repetitive pattern in, what appears to be, the "steady state" response to the single harmonic input motion. Note that the experimental work contained only a fraction of high harmonics recorded at base (the discussion provides further comments on this aspect), whereas the numerically applied input motion contained solely 10Hz frequency. The pattern of high frequency motion registered experimentally on piles is not fully consistent with respect to those predicted by the simulations. Potential reasons for such discrepancy could lie in the approximately evaluated mass of the measuring devices placed on the top of the pile in the numerical study or plastic shear strain accumulation in soil in the experimental work due to the numerous dynamic tests performed on the same soil specimen (thus possibly affecting the response of the piles embedded in soil). Nevertheless, the fact of observing high frequency motion on the piles in the numerical and experimental studies, even if of inconsistent patterns, can be considered as further potential evidence supporting the idea that high frequency motion can be generated in nonlinear hysteretic soil and affect the structural response. In other words, the pile with a mass on its top can be thought to be an "elastic inclusion" placed in soil and acting as additional measuring instrumentation able to pick up and amplify the high frequency motion generated in the soil mass.

4. Discussion

The result section has presented introductory consideration supporting the hypothetical idea of the phenomenon of the release of soil elastic waves in nonlinear hysteretic soil. The occurrence of elastic waves has been shown to result in the observation of high frequency motion in the dynamic response of soil. These results, if confirmed in more detailed research in the future, in the opinion of the Authors, may have significant importance on various aspects of earthquake geotechnical engineering and beyond. These aspects could include: pointing out gaps in the theory of wave propagation, recognizing a possible unknown new origin of high frequency motion measured in small-scale experiments, understanding the source of very high frequency numerical noise in finite element numerical analyses, showing new insights on seismic soil-structure interaction and, finally, possibly casting new light on stress wave propagation in soil in real earthquakes.

First of all, this study shows potential gaps in the theory of wave propagation. In the light of no analytical solution for the wave propagation problems in the nonlinear hysteretic materials, the wave propagation has been investigated in this work by means of a simplified soil constitutive model in the framework of the finite element method. To the best of the Authors' knowledge, the release and the "entrapment" of soil elastic waves has not been shown before in the stress wave propagation problems. Note that the numerical studies presented in Section 3 have chosen depth dependent material definitions to be representative of real soil behaviour. Nevertheless, the release of elastic waves can also be shown in depth independent materials in a column of a finite height, thus the presented phenomenon would be applicable to general mechanics and physics. This fact has been omitted in this work for the sake of compliance with the real soil behaviour and the direct applicability of the obtained results to the experimental observations, however future works could address more general cases of wave

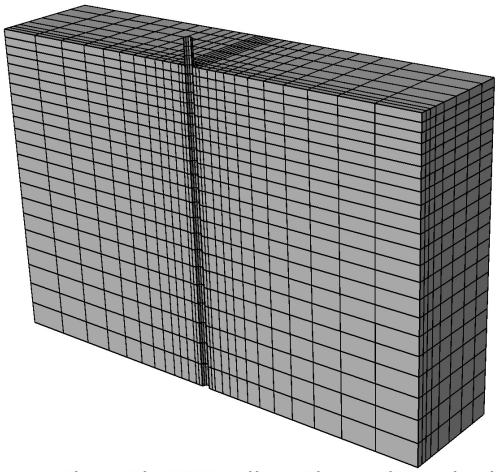

Figure 17. Mesh discretization of the boundary value problem of the soil-structure interaction.

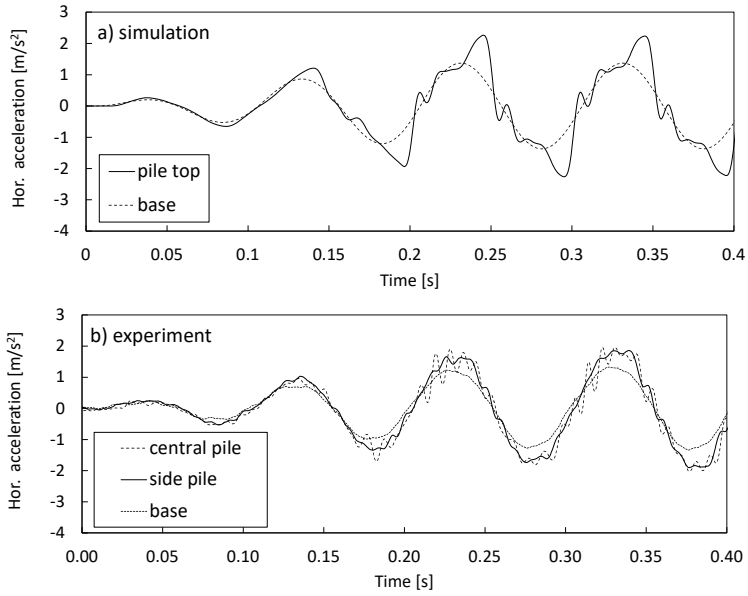

Figure 18. Comparison of the horizontal accelerations computed and recorded in the boundary value problem: a) numerical simulation, b) experimental data.

propagation, including wave propagation in finite elastic bodies.

The presented hypothetical idea of the release of soil elastic waves in nonlinear hysteretic soil may cast new light on the potential source of high frequency motion registered often in experimental works when a soil specimen is subjected to simplified sinusoidal input motions. Some explanation to the occurrence of the high harmonics in the evaluated spectral responses was pointed out in the past towards soil non-linearity which results in the distortion of a sine wave towards a square wave (e.g. [Mercado et al., 2018]). Nevertheless, apparently experimental works do not register high frequency components with the pattern of an exponential decay (i.e. representative of the distortion towards a square wave). In the opinion of the Authors, such wave distortion towards a square wave would not lead experimentalists to filter experimental measurements. Moreover, the numerical studies of this work suggest that higher harmonics may not be limited to those below 80Hz as shown in the experiments [Durante, 2015]. Thus, it would be interesting to avoid filtering or to filter experimental data with a higher cut-off frequency in future works, in order to validate the speculative part of the findings presented in this paper.

A single case of the numerical analysis in Section 3 is compared with the experiments conducted by Dar [1993]. These experiments were often characterized by double-peak acceleration records in soil in the top part of the soil container when subjected to high amplitude input motions (i.e higher than 0.15g used in the work by Durante [2015]). Originally, the explanation of such double peaks was attributed to "soil fluidisation" potentially taking place in soil [Dar, 1993] or later, possibly to strain localisation due to the development of a shear band [Gajo and Muir Wood, 1997].

The latter was suggested even though the maximum lateral displacements were reported to be around 2-3mm [Gajo and Muir Wood, 1997], thus possibly too low to represent the shear band development. In addition to the peculiarities observed in the horizontal accelerations, some further unrecognized phenomena on soil surface were observed in the vertical displacements measured by Dar [1993] and Durante [2015] as mentioned by Gajo and Muir Wood [1997] and Kowalczyk [2020], respectively. These irregularities could be related to the strain localisation [Gajo and Muir Wood, 1997] or be representative of the soil-released elastic waves "trapped" in the soil specimen. Clear distinction on whether strain localisation, soil elastic waves, or combination of these phenomena leads to double peaks in the horizontal accelerations at soil surface under high amplitude input motions, could be confirmed in future dedicated experimental works.

Importantly, regarding experiments in flexible soil containers, some consideration is worth to be given to the recorded input motions in experimental works. Namely, a difference between small-scale tests performed at 1g (e.g. [Durante, 2015]) and in centrifuge (e.g. [Madabhushi et al., 2020]) is sometimes observed in terms of the recorded input motions at base. In particular, high harmonics are apparently more prominent at base in centrifuge tests, notwithstanding the intended input motion should consist only of a single harmonic. For this reason, the high frequencies are sometimes considered to be generated by the actuator itself (e.g. [Brennan et al., 2005], [Yao et al., 2017]). The possibility that the high harmonics at base are due to the actuators themselves cannot be excluded. This, indeed, might be the case in centrifuges at certain geotechnical research centres (e.g. [Kutter et al., 2018]). On the other hand, it is worth observing that, the soil specimen in a soil container placed on a shaking table are one complex dynamic system, in which energy induced by the actuators is reflected from the soil specimen back to the shaking table and its actuators. Moreover, the differences between the dynamic impedance of the soil specimen in soil containers on shaking tables are expected to vary in a wide range for various experimental setups, especially in 1g apparatuses as compared to the apparatuses in centrifuge tests (for obvious reasons of payload). Thus, the high frequency motion generated within the soil mass is expected to have different effects on "heavy" 1g experimental setups (as the ones used herein for comparisons) with respect to the "light" centrifuge setups, potentially inducing unwanted high frequency motion even at the level of the shaking table and controlling systems.

This work has revealed potential new source of the high frequency motion observed in experimental setups subjected to sinusoidal input motions, in addition to those already suggested long time ago (e.g. strain localisation) or more recently (e.g. separation of the elastic part of the wave from the plastic part [Kowalczyk, 2020]). The latter phenomenon can take place when there is a non-smooth change in the soil stiffness between the elastic and the plastic part of the mechanical behaviour. This might be the case of soil, especially when we recall that the elastic behaviour is associated often with an undisturbed soil fabric, whereas plastic behaviour is associated with changes in the soil fabric. Therefore, intuitively it may appear possible that such initiation of change in soil fabric may result in a non-perfectly-smooth transition between the elastic and plastic stiffnesses, thus allowing separation of the elastic precursor wave resulting in the "entrapment" of separated soil elastic waves. Although this phenomenon was indicated as potentially possible to occur in soil specimens placed in flexible soil containers [Kowalczyk, 2020], this work shows that the release of soil elastic waves would rather be dominant in small-scale experimental studies. On the other hand, in real earthquakes, the separation of the elastic precursor cannot be excluded. Nevertheless, this has not been a subject of further consideration in this paper.

The results in this paper are mainly related to simplified input motions used in the numerical and experimental studies. On the other hand, one may want to ask if soil elastic waves can also be released in real earthquakes. Some indication to this point has been shown in Section 3 of this paper where scaled earthquake input motion was analysed and revealed potential presence of soil elastic waves. Indeed, the results shown in this paper can contribute to the discussion of double-peak spectra earthquakes (e.g. [Gallegos and Saragoni, 2017]) where the two peaks are attributed to represent the source (i.e. the driving frequency) and the site (i.e. the soil natural frequency) response. Our work suggests that the response of a site bounded at base by a stratum of large stiffness contrast may be heavily affected by soil released elastic waves "trapped" in this stratum. In fact, the origins of what was identified as higher modes of free vibrations in some earthquakes [Ruiz and Saragoni, 2009], including the site of Mexico City, has not been recognized. Regarding the seismic response of Mexico City, where a soft clay layer is bounded by rock at base, there is a number of observations which is not consistently explained. These observations include anomalous records on the rock sites contaminated by unexpected long-period vibrations or unusually long duration of motion in the soft clay layer characterized usually by monochromatic vibrations, thus by the possible presence of soil elastic waves (e.g. records on the soft clay observed at station Aux as shown recently by Garini et al. [2022]). According to some previous research works (e.g. [Singh et al., 1995]) the anomalous records on the rock sites could be representative of the underlying stratigraphy of low-velocity layers. Nevertheless, based on the findings in this work, an alternative explanation of the anomalous records on the rock sites could be speculated. Namely, the anomalies may possibly be representative of the overlying stratigraphy, i.e. the soft clay soil layer in the lake basin, where soil elastic wave may be generated and "trapped" as in the case of the simplified numerical studies of the soil container.

The present work has also important implications on the numerical modelling of soil response under dynamic excitation. It has been shown that the standard formulation of the finite element method encounters difficulties in representing the propagation of soil elastic waves for relatively

large amplitude motions where strong strain discontinuity occurs. This strain discontinuity causes generation of spurious very high frequency numerical oscillations in the computed strains and accelerations. The presence of soil elastic waves can explain the numerical difficulties that are typically encountered in computational modelling of seismic geotechnical problems. In any case, the occurrence of strain discontinuity due to the release of elastic waves might demand the use of more sophisticated numerical techniques (such as the discontinuous Galerkin method, higher order finite elements, e.g. [Semblat and Brioist, 2000]; or Godunov's method, e.g. [Fellin, 2002]) than those currently used in practice and employed in this work. It would be presumed that the use of such techniques would allow for further developments of the numerical findings shown in this paper, for example when identifying when in a loading cycle and where in a soil column, the elastic waves are released. Moreover, the simplified constitutive approach, although useful in identifying basic constitutive features needed to observe the release of soil elastic waves, may not be fully suitable for replicating complex soil behaviour. In addition, this work may point out on the importance of two other aspects in soil numerical modelling. The first one is the appropriate definition of the initial elastic soil stiffness by soil constitutive models. Only soil constitutive models which define the very small strain initial stiffness in a reliable way, can be expected to compute accurately the soil response with soil elastic waves. The second numerical aspect to consider carefully is the amount of viscous damping often used in numerical studies. It has not been shown in this work, however excessively large viscous damping may remove any high frequency motion from the computations including the one representing soil elastic waves.

This study has presented initial, mainly numerical and some potential experimental, evidence supporting the hypothetical idea of the release of soil elastic waves in nonlinear hysteretic soil. The presented results have been based on s-wave propagation in dry soil. In the light of a substantial number of recent experimental works dealing with saturated soil and liquefaction cases, the Authors of this work were somehow "lucky" to have access to examples of the experimental research carried out in dry sand. Thus, the numerical studies herein were developed for dry sand where the apparent "steady state"-like response under harmonic motion can be reached. Nevertheless, the release of soil elastic waves would equally be expected in the response of saturated soil. However, in that case, the "steady state"-like response under harmonic excitation is typically not reached due to the ongoing significant changes in the stiffness of saturated soil as a result of pore pressure generation, thus the release of soil elastic waves is expected to be much more difficult to be recognized.

Finally, it has to be recalled that, although the numerical studies have rather convincingly identified the release of soil elastic waves, the experimental examples used here for the purpose of comparisons with the numerical studies are more uncertain. In fact, these experimental works were focused on other aspects of soil dynamic response (i.e. the response of piles in [Durante, 2015] or the development of a flexible soil container in [Dar, 1993]). Moreover, these works could also be influenced by other phenomena resulting in the observation of high frequency motion, e.g. wave reflections due to a bi-layered soil profile or wave scattering from the piles in the work of Durante [2015], or shear band development in the work of Dar [1993]. Therefore, it appears that there is need for further investigation of the presented idea, including experimental studies dedicated towards clear confirmation of the potential existence of soil elastic waves in the dynamic response of soil.

5. Conclusions

This paper presented initial consideration supporting the hypothetical idea of the release of soil elastic waves in nonlinear hysteretic soil, mainly when subjected to harmonic excitation, but also possibly in the response to earthquake motion. The potential release of soil elastic waves in nonlinear hysteretic soil was shown, primarily, in the simplified finite element numerical simulations, and secondarily, by comparisons with past experimental works on shaking tables. The paper showed that soil elastic waves can be a potential explanation to high frequency components registered often in experimental works and can possibly be important in real earthquakes and when analysing structural response in experimental works.

CRediT authorship contribution statement

Piotr Kowalczyk: Conceptualisation (equal), Methodology (equal), Software (supporting), Formal analysis, Investigation (lead), Resources (supporting), Data curation, Writing -original draft, Writing -review and editing (lead), Visualisation, Funding acquisition (lead). **Alessandro Gajo**: Conceptualisation (equal), Methodology (equal), Software (lead), Investigation (supporting), Resources (lead), Writing -review and editing (supporting), Funding acquisition (supporting).

Conflicts of Interest

The authors declare no conflicts of interest. The complete review history is available online.

Acknowledgements

The research presented herein has been initiated as a part of a EU-funded project under the European Union's Horizon 2020 research and innovation programme, grant agreement No 721816.

The Authors would like to thank Professor Colin Taylor (University of Bristol, UK) for his insightful remarks regarding the complexity of physical modelling of soil behaviour in small-scale experiments.

The Authors would like to gratefully acknowledge the provision of examples of raw experimental data of the small-scale experimental work on piles by Dr Maria Giovanna Durante (University of Calabria, Italy) and Professor Luigi Di Sarno (University of Liverpool, UK).

The Authors would also like to thank the three Reviewers for their constructive remarks and valuable comments on this paper.

The first Author would like to acknowledge using computational resources of University of Southampton (UK) for the revision stage of this work.

Appendix A. Calibration of the simplified soil constitutive model

This appendix presents briefly the calibration approach of the simplified soil constitutive model (1) to ensure reasonably realistic simulation of experimental works in flexible soil containers. The calibration of the model parameters was such that: 1) the initial G_0 profile with depth reflected the empirical evaluation by Hardin and Drnevich [1972], 2) the stiffness degradation G/G_0 was in line with the recommendations given by Dietz and Muir Wood [2007] and the limits by Seed and Idriss [1970]. These recommendations were specified for deformation in simple shear in low mean effective stresses, i.e. representative of dominant stress path experienced by soil in flexible soil containers. The used empirical expression for the evaluation of the initial G_0 profile is given below:

$$G_0 = \frac{3230 \cdot (2.97 - e)^2 \cdot \sqrt{p'}}{(1 + e)} \tag{3}$$

For the majority of the numerical simulations the model parameters where calibrated to reflect experimental setup of Durante [2015], thus density ρ of 1332 kg/m^3, K_0=0.5, e=0.9 have been assumed as per the experiment. The shear stiffness G_0 profile was plotted in Figure 2 whereas stiffness degradation G/G_0 in Figure A.1. Furthermore, to replicate numerically the experimental setup by Dar [1993] the computed G_0 profile was calibrated following the experimental assumptions and measurements (density ρ of 1700kg/m^3, K_0=0.6, e=0.6 by Dar [1993]) and it is shown in Figure A.2. Finally, the shear stiffness degradation for the single numerical simulation of Dar's experiment is shown in Figure A.3.

Appendix B. Ormsby wavelet identification

This appendix presents the numerical dynamic identification of an 0.8m high soil column modelled with a simplified constitutive model (1). The chosen input motion is an Ormsby wavelet (Figure B.1a) of a flat spectral response between 10Hz and 110Hz (Figure B.1b) and the maximum amplitude of 0.0001g. The soil column subjected to such input motion responses at its top as shown in Figure B.1c. The evaluated first two natural frequencies of the soil column are around 33.0Hz and 88.5Hz (Figure B.1d).

Table C.1. Input parameters for the Severn-Trent sand model

Parameter	Description	Value
v_Δ	Intercept for critical-state line in v-ln p plane at p=1Pa	2.194
Δ	Slope of critical-state line in v-ln p plane	0.0267
ϕ_{cv}	Critical-state angle of friction	33°
m	Parameter controlling deviatoric section of yield surface	0.8
k	Link between changes in state parameter and current size of yield surface	3.5
A	Multiplier in the flow rule	0.75
k_d	State parameter contribution in flow rule	1.3
B_{min}	Parameter controlling hyperbolic stiffness relationship	0.0005
B_{max}	Parameter controlling hyperbolic stiffness relationship	0.002
α	Exponent controlling hyperbolic stiffness relationship	1.6
R_R	Size of the yield surface with respect to the strength surface	0.02
E_R	Fraction of G_0 used in the computations	1.0

Appendix C. Calibration and performance of the advanced soil constitutive model

This appendix presents the input parameters (Table C.1), the fit of the chosen calibration (Figure C.1) of the Severn-Trent sand constitutive model together with an example of its response when simulating a cyclic simple shear test on Toyoura Sand compared with experimental data [Shahnazari and Towhata, 2002] shown in Figure C.2.

References

Abate, G. and Massimino, M. R. (2016). Dynamic soil-structure interaction analysis by experimental and numerical analysis. *Riv. Ital. Geot.*, 2:44–70.

Been, K. and Jefferies, M. J. (1985). A state parameter for sands. *Géotechnique*, 35(2):99–112.

Bilotta, E., Lanzano, G., Madabhushi, S. P. G., and Silvestri, F. (2014). A numerical Round Robin on tunnels under seismic actions. *Acta Geot.*, 9:563–579.

Bonilla, L. F., Archuleta, R. J., and Lavallée, D. (2005). Hysteretic and dilatant behaviour of cohesionless soils and

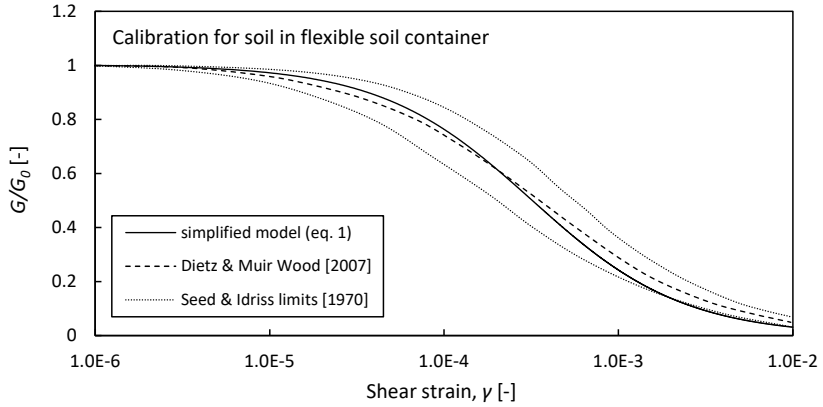

Figure A.1. Calibration of the simplified soil constitutive model (1) for the experimental setup of Durante [2015] compared with the guidelines by Dietz and Muir Wood [2007] and Seed and Idriss [1970] for simple shear deformation in low mean effective stresses in flexible soil containers.

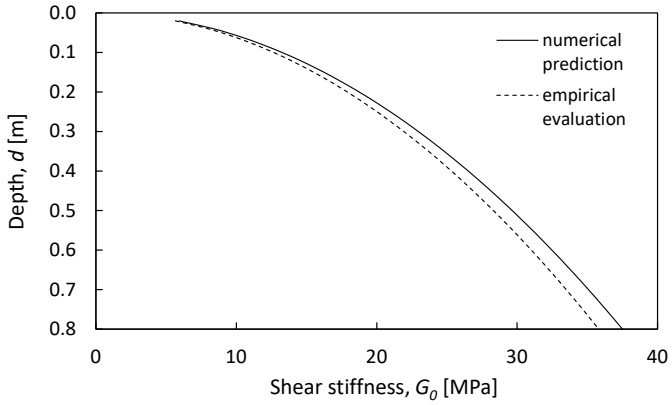

Figure A.2. Calibration of the simplified soil constitutive model (1) for the experimental setup of Dar [1993] in terms the initial G_0 profile.

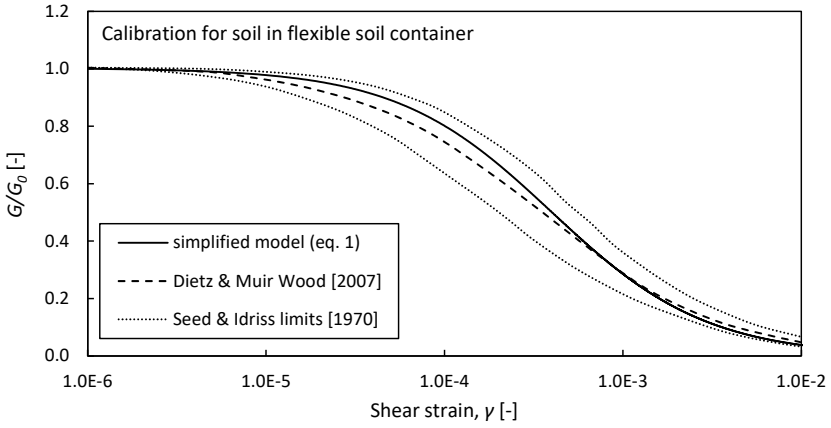

Figure A.3. Calibration of the simplified soil constitutive model (1) for the experimental setup of Dar [1993] compared with the guidelines by Dietz and Muir Wood [2007] and Seed and Idriss [1970] for simple shear deformation in low mean effective stresses in flexible soil containers.

their effects on nonlinear soil response: field data observations and modelling. *Bull. Seism. Soc. Am.*, 95(6):2373–2395.

Brennan, A. J., Thusyanthan, N. I., and Madabhushi, S. P. G. (2005). Evaluation of shear modulus and damping in dynamic centrifuge tests. *J. Geot. Geoenv. Eng.*, 131(12):1488–1497.

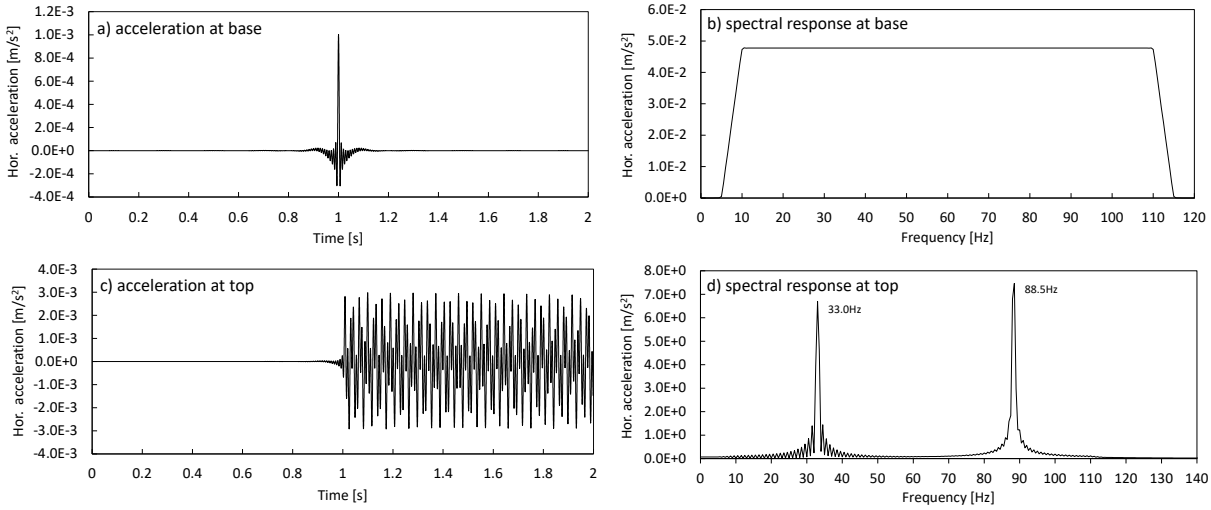

Figure B.1. Dynamic identification by means of an Ormsby wavelet of the 0.8m high soil column modelled with the simplified constitutive law (1): a) input horizontal acceleration at base (i.e. Ormsby wavelet), b) evaluated spectral response at base, c) computed horizontal acceleration at top, d) evaluated spectral response at top.

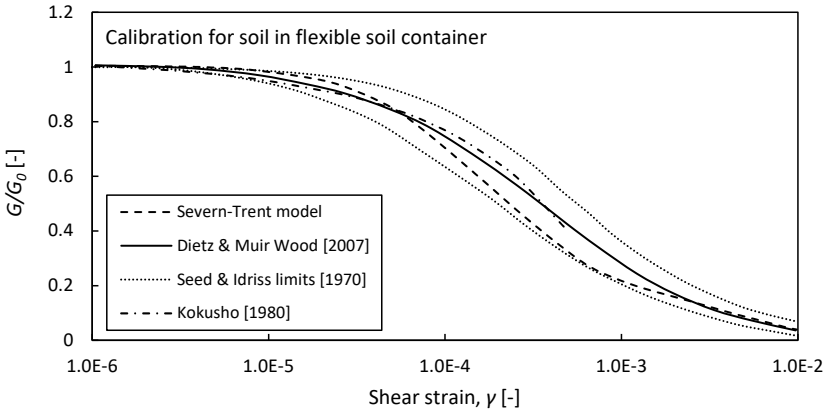

Figure C.1. Calibration of the advanced elastoplastic soil constitutive model compared with the guidelines by Dietz and Muir Wood [2007], Seed and Idriss limits [Seed and Idriss, 1970] and laboratory data by Kokusho [1980] for simple shear deformation in low mean effective stresses in flexible soil containers.

Chau, K. T., Shen, C. Y., and Guo, X. (2009). Nonlinear seismic soil-pile-structure interactions: Shaking table tests and FEM analyses. *Soil Dyn. Earthq. Eng.*, 29:300–310.

Conti, R., Madabhushi, G. S. P., and Viggiani, G. M. B. (2012). On the behaviour of flexible retaining walls under seismic actions. *Géotechnique*, 62(12):1081–1094.

Conti, R. and Viggiani, G. M. B. (2012). Evaluation of Soil Dynamic Properties in Centrifuge Tests. *J. Geot. Geoenv. Eng.*, 138(7):850–859.

Dafalias, Y. F. and Manzari, M. T. (2004). A simple plasticity sand model accounting for fabric change effects. *J. Eng. Mech.*, 130(6):622–634.

Dar, A. R. (1993). *Development of a flexible shear-stack for shaking table testing of geotechnical problems*. PhD thesis, University of Bristol.

Dassault Systèmes (2019). Abaqus Standard software package.

Dietz, M. and Muir Wood, D. (2007). Shaking table evaluation of dynamic soil properties. In *Proceedings of 4th International Conference of Earthquake Geotechnical Engineering, June 25-28, Thessaloniki, Greece*, pages 25–28.

Durante, M. G. (2015). *Experimental and numerical assessment of dynamic soil-pile-structure interaction*. PhD thesis, Università degli Studi di Napoli Federico II, Italy.

Durante, M. G., Di Sarno, L., Mylonakis, G., Taylor, C. A., and Simonelli, A. L. (2016). Soil-pile-structure interaction: experimental outcomes from shaking table tests. *Earthq. Eng. Struct. Dyn.*, 45(7):1041–1061.

Fan, F. G., Ahmadi, G., and Tadjbakhsh, I. G. (1988). Base isolation of a multi-story building under a harmonic ground motion - a comparison of performances of various systems. Technical Report NCEER-88-0010.

Fellin, W. (2002). Numerical computation of nonlinear inelastic waves in soils. *Pure Appl. Geophys.*, 159:1737–1748.

Gajo, A. (2010). Hyperelastic modelling of small-strain anisotropy of cyclically loaded sand. *Int. J. Numer. Anal.*

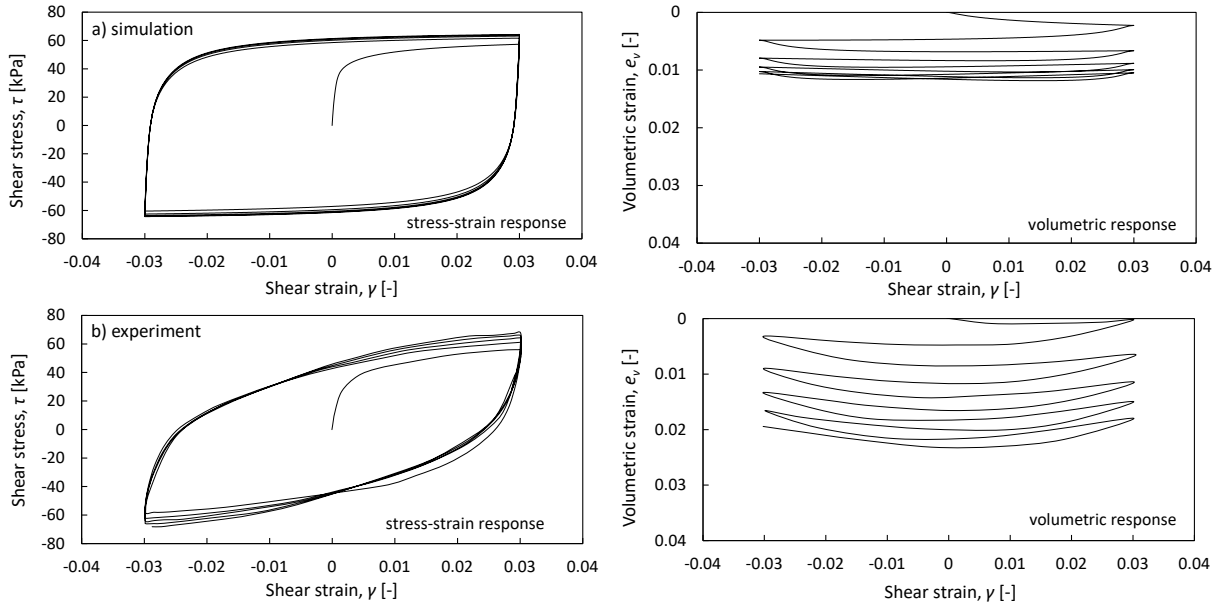

Figure C.2. Typical responses of the Severn-Trent sand model in simulation of a drained cyclic simple shear test on loose sand compared with laboratory results ($p' = 98$kPa, $e_0 = 0.756$): a) numerical simulation, b) experiments by Shahnazari and Towhata [2002].

Methods Geomech., 34(2):111–134.

Gajo, A. and Muir Wood, D. (1997). Numerical analyses of behaviour of shear stacks under dynamic loading. Report on work performed under the EC project European Consortium of Earthquake Shaking Tables (ECOEST): Seismic bearing capacity of shallow foundations.

Gajo, A. and Muir Wood, D. (1999a). A kinematic hardening constitutive model for sands: the multiaxial formulation. *Int. J. Numer. Anal. Methods Geomech.*, 23(9):925–965.

Gajo, A. and Muir Wood, D. (1999b). Severn-Trent sand: a kinematic hardening constitutive model for sands: the q-p formulation. *Géotechnique*, 49(5):595–614.

Gallegos, M. F. and Saragoni, G. R. (2017). Analysis of strong-motion accelerograph records of the 16 April 2016, Mw 7.8 Muisne, Ecuador Earthquake. In *Proceedings of 16th World Conference on Earthquake Engineering, Santiago, Chile*.

Garini, E., Anastasopoulos, I., Gazetas, G., O'Riordan, N., Kumar, P., Ellison, K., and Ciruela-Ochoa, F. (2022). Discussion on: Soil, basin and soil-building-soil interaction effects on motions of Mexico City during seven earthquakes. *Géotechnique*, 72(6):556–564.

Hardin, B. O. and Drnevich, V. P. (1972). Shear modulus and damping in soils. *J. Soil Mech. Found. Div.*, 98(7):667–692.

Kelly, J. M. (1982). The influence of base isolation on the seismic response of light secondary equipment. Research Report UCB/EERC-81/17. University of California, Berkeley.

Kokusho, T. (1980). Cyclic triaxial test of dynamic soil properties for wide strain range. *Soils Found.*, 20(2):45–60.

Kowalczyk, P. (2020). *Validation and application of advanced soil constitutive models in numerical modelling of soil and soil-structure interaction under seismic loading*. PhD thesis, University of Trento, Italy.

Kramer, S. L. (1996). *Geotechnical Earthquake Engineering*. Prentice Hall.

Kutter, B. L., Carey, T. J., Hashimoto, T., Zeghal, M., Abdoun, T., Kokkali, P., Madabhushi, G. S. P., Haigh, S. K., Burali d'Arezzo, F., Madabhushi, S. S. C., Hung, W.-Y., Lee, C.-J., Cheng, H.-C., Iai, S., Tobita, T., Ashino, T., Ren, J., Zhou, Y.-G., Chen, Y.-M., Sun, Z.-B., and Manzari, M. T. (2018). Leap-GWU-2015 experiment specifications, results and comparisons. *Soil Dyn. Earthq. Eng.*, 113:616–628.

Kutter, B. L., Carey, T. J., Stone, N., Li Zheng, B., Gavras, A., Manzari, M. T., Zeghal, M., Abdoun, T., Korre, E., Escoffier, S., Haigh, S. K., Madabhushi, G. S. P., Madabhushi, S. S. C., Hung, W.-Y., Liao, T.-W., Kim, D.-S., Kim, S.-N., Ha, J.-G., Kim, N. R., Okamura, M., Sjafruddin, A. N., Tobita, T., Ueda, K., Vargas, R., Zhou, Y.-G., and Liu, K. (2019). *LEAP-UCD-2017 Comparison of Centrifuge Test Results*. Springer.

Kutter, B. L. and Wilson, D. W. (1999). De-liquefaction shock waves. In *Proceedings of 7th U.S.-Japan Workshop on Earthquake Resistant Design for Lifeline Facilities and Countermeasures Against Soil Liquefaction*, pages 295–310. Technical Report MCEER-99-0019.

Lanzano, G., Bilotta, E., Russo, G., Silvestri, F., and Madabhushi, S. P. G. (2012). Centrifuge modelling of seismic loading on tunnels in sand. *Geot. Testing J.*, 35(6):854–869.

Madabhushi, G. S. P. (2014). *Centrifuge modelling for civil engineers*. Taylor & Francis.

Madabhushi, S. S. C., Dobrisan, A., Beber, R., Haigh, S. K., and Madabhushi, G. S. P. (2020). Leap-UCD-2017 Centrifuge tests at Cambridge. In Kutter, B., Manzari, M., and Zeghal, M., editors, *Model Tests and Numerical Simulations of Liquefaction and Lateral Spreading*. Springer.

Manandhar, S., Kim, S.-N., Ha, J.-G., Ko, K.-W., Lee, M.-G., and Kim, D.-S. (2021). Liquefaction evaluation using frequency characteristics of acceleration records in KAIST

centrifuge tests for LEAP. *Soil Dyn. Earthq. Eng.*, 140.

Manzari, M. T., El Ghoraiby, M., Zeghal, M., Kutter, B. L., Arduino, P., Barrero, A. R., Bilotta, E., Chen, L., Chen, R., Chiaradonna, A., Elgamal, A., Fasano, G., Fukutake, K., Fuentes, W., Ghofrani, A., Haigh, S. K., Hung, W.-Y., Ichii, K., Kim, D. S., Kiriyama, T., Lascarro, C., Madabhushi, G. S. P., Mercado, V., Montgomery, J., Okamura, M., Ozutsumi, O., Qiu, Z., Taiebat, M., Tobita, T., Travasarou, T., Tsiaousi, D., Ueda, K., Ugalde, J., Wada, T., Wang, R., Yang, M., Zhang, J.-M., Zhou, Y.-G., and Ziotopoulou, K. (2019). Leap-2017: Comparison of the Type-B Numerical Simulations with Centrifuge Test Results. In Kutter, B. et al., editors, *Model tests and numerical simulations of liquefaction and lateral spreading: LEAP-UCD-2017*, pages –2017. Springer.

McAllister, G., Taiebat, M., Ghofrani, A., Chen, L., and Arduino, P. (2015). Nonlinear site response analyses and high frequency dilation pulses. In *Proceedings of 68th Canadian Geotechnical Conference (Quebec, Canada)*.

Mercado, V., El-Sekelly, W., Abdoun, T., and Pajaro, C. (2018). A study on the effect of material nonlinearity on the generation of frequency harmonics in the response of excited soil deposits. *Soil Dyn. Earthq. Eng.*, 115:787–798.

Nekorkin, V. (2015). *Introduction to nonlinear oscillations*. John Wiley & Sons.

Niemunis, A. and Herle, I. (1997). Hypoplastic model for cohesionless soils with elastic strain range. *Mech. Cohesive-Frictional Mater.*, 2:279–299.

Nowacki, W. K. (1978). *Stress waves in non-elastic solids*. Pergamon Press.

Pavlenko, O. (2001). Nonlinear seismic effects in soils: numerical simulation and study. *Bull. Seism. Soc. Am.*, 91(2):381–396.

Pavlenko, O. and Irikura, K. (2005). Identification of the nonlinear behaviour of liquefied and non-liquefied soils during the 1995 Kobe earthquake. *Geophys. J. Int.*, 160(2):539–553.

Roten, D., Fah, D., and Bonilla, L. F. (2013). High-frequency ground motion amplification during the 2011 Tohoku earthquake explained by soil dilatancy. *Geophys. J. Int.*, 193(2):898–904.

Ruiz, S. and Saragoni, G. R. (2009). Free vibrations of soil during large earthquakes. *Soil Dyn. Earthq. Eng.*, 29(1):1–16.

Seed, H. B. and Idriss, I. M. (1970). Soil moduli and damping factors for dynamic response analysis. EERC report 70-10. University of California, Berkeley.

Semblat, J. F. and Brioist, J. J. (2000). Efficiency of higher order finite elements for the analysis of seismic wave propagation. *J. Sound Vib.*, 231(2):460–467.

Shahnazari, H. and Towhata, I. (2002). Torsion shear tests on cyclic stress-dilatancy relationship of sand. *Soils Found.*, 42(1):105–119.

Singh, S. K., Quaas, R., Ordaz, M., Mooser, F., Almora, D., Torres, M., and Vasquez, R. (1995). Is there truly a "hard" rock site in the Valley of Mexico? *Geophys. Res. Lett.*, 22(4):481–484.

Song, E. X., Haider, A., and Peng, L. (2018). Numerical simulation of plane wave propagation in a semi-infinite media with a linear hardening plastic constitutive model. In *Proceedings of China-Europe Conference on Geotechnical Engineering*, volume 1 of *Springer Series in Geomechanics and Geoengineering*, pages 410–414. Springer.

Tsiapas, Y. Z. and Bouckovalas, G. D. (2018). Selective Filtering of Numerical Noise in Liquefiable Site Response Analyses. In *Proceedings of Geotechnical Earthquake Engineering and Soil Dynamics Conference, June 10-13, Austin, Texas*, pages 10–13.

Veeraraghavan, S., Spears, R. E., and Coleman, J. L. (2019). High frequency content in soil nonlinear response: A numerical artefact or a reality? *Soil Dyn. Earthq. Eng.*, 116:185–191.

Vitorino, M. V., Vieira, A., and Rodrigues, M. S. (2017). Effect of sliding friction in harmonic oscillators. *Sci. Rep.*, 7(1):3726.

Von Wolffersdorff, P. A. (1996). A hypoplastic relation for granular materials with a predefined limit state surface. *Mech. Cohesive-Frictional Mater.*, 1(3):251–271.

Wang, G., Wei, X., and Zhao, J. (2018). Modelling spiky acceleration response of dilative sand deposits during earthquakes with emphasis on large post-liquefaction deformation. *Earthq. Eng. Eng. Vib.*, 17(1):125–138.

Wang, L. (2007). *Foundations of stress waves*. Elsevier.

Watanabe, K., Pisano, F., and Jeremic, B. (2017). Discretization effects in the finite element simulation of seismic waves in elastic and elastic-plastic media. *Eng. Comput.*, 33:519–545.

Wiebe, L. and Christopoulos, C. (2010). Characterizing acceleration spikes due to stiffness changes in nonlinear systems. *Earthq. Eng. Struct. Dyn.*, 39:1653–1670.

Yao, J., Han, Y., Dietz, M., Xiao, R., Chen, S., Wang, T., and Niu, Q. (2017). Acceleration harmonic estimation for a hydraulic shaking table by using particle swarm optimization. *Trans. Inst. Meas. Control*, 39(5):738–747.

Manuscript received 6th December 2022, revised 22nd June 2023, accepted 5th July 2023.